Geochimica et Cosmochimica Acta, Vol. 69, No. 24, pp. 5659–5680, 2005

0016-7037/05 $30.00 + .00

doi:10.1016/j.gca.2005.07.018

Basalt weathering in Central Siberia under permafrost conditions

O. S. Pokrovsky,[1,*] J. Schott,[1] D. I. Kudryavtzev,[2] and B. Dupré[1]

[1]Laboratoire des Mécanismes et Transfert en Geologie (LMTG), UMR 5563, CNRS-UPS-IRD OMP, 14 Avenue Edouard Belin, 31400 Toulouse, France

[2]Geological Institute (GIN) Russian Academy of Science, Puzhevsky Per. 7, 119017 Moscow, Russia

(*Received March* 28, 2005; *accepted in revised form July* 25, 2005)

Abstract—Chemical weathering of basalts in the Putorana Plateau, Central Siberia, has been studied by combining chemical and mineralogical analysis of solids (rocks, soils, river sediments, and suspended matter) and fluid solution chemistry. Altogether, 70 large and small rivers, 30 soil pore waters and groundwaters and over 30 solids were sampled during July to August 2001. Analysis of multiannual data on discharge and chemical composition of several rivers of the region available from the Russian Hydrological Survey allowed rigorous estimation of mean annual major element concentrations, and dissolved and suspended fluxes associated with basalt weathering. For the rivers Tembenchi and Taimura that drain monolithologic basic volcanic rocks, the mean multiannual flux of total dissolved cations (TDS_c = Ca + Mg + Na + K) corrected for atmospheric input is 5.7 ± 0.5 t/km^2/yr. For the largest river Nizhniya Tunguska—draining essentially basic rocks—the TDS_c is 6.1 ± 1.5 t/km^2/yr. The overall CO_2 consumption flux associated with basalt weathering in the studied region (~700,000 km^2) achieves 0.08×10^{12} mol/yr, which represents only 2.6% of the total CO_2 consumption associated with basalt weathering at the Earth's surface. The fluxes of suspended matter were estimated as 3.1 ± 0.5, 9.0 ± 0.8, and 6.5 ± 2.0 t/km^2/yr for rivers Taimura, Eratchimo, and Nizhniya Tunguska, respectively. Based on chemical analyses of river solutes and suspended matter, the relative dissolved versus particulate annual transport of major components is $C_{inorg} \geq C_{org} > Na + K > Ca > Mg > Si > Fe \geq Mn \geq Ti \geq Al$ which reflects the usual order of element mobility during weathering.

According to chemical and mineralogical soil and sediment analyses, alteration of basalt consists of (1) replacement of the original basaltic glass by Si-Al-Fe rich amorphous material, (2) mechanical desegregation and grinding of parent rocks, leading to accumulation of "primary" hydrothermal trioctahedral smectite, and (3) transformation of these trioctahedral (oxy)smectites and mixed-layer chlorite-smectite, into secondary dioctahedral smectite accompanied by removal of Ca, Mg, and Fe, and enrichment in Al. No vertical chemical differentiation of fluid and solid phases within the soil profile was identified. All sampled soil pore waters and groundwaters were found to be close to equilibrium with respect to chalcedony, gibbsite, halloysite, and allophanes, but strongly supersaturated with respect to goethite, nontronite, and montmorillonite.

Over the annual cycle, the contribution of atmospheric precipitation, permafrost melting, underground reservoirs, litter degradation, and rock and soil mineral weathering for the overall TDS_c transport in the largest river of the region (Nizhniya Tunguska) is 9.3 ± 3, 10 ± 5, 10.5 ± 5, 25 ± 20, and 45 ± 30%, respectively. In the summertime, direct contribution of rocks and soil mineral weathering via solid/fluid interaction does not exceed 20%. The main unknown factors of element mobilization from basalt to the river is litter degradation in the upper soil horizon and parameters of element turnover in the vegetation.

1. INTRODUCTION

Chemical weathering of silicate rocks is considered to be the principal process removing carbon dioxide from the atmosphere on long timescales (Berner, 1992), with the alteration of continental basalts accounting for ~30% of CO_2 total consumption (Dupré et al., 2003). As a result, numerous studies have been devoted to characterizing basalt weathering both from the analysis of soils and rocks, and from river solution chemistry (Nesbitt and Wilson, 1992; Gislason et al., 1996; Stefansson and Gislason, 2001 and references therein). These studies allowed the extraction of a quantitative picture of basalt weathering in various climates and determined the major factors controlling the intensity of chemical weathering. Runoff, temperature, rock mineralogy, and vegetation have been listed among the most important parameters governing the overall chemical erosion of basalts (Benedetti et al., 1994; Drever, 1994; White and Blum, 1995; Gislason et al., 1996; Brady et al., 1999; Moulton et al., 2000; Dessert et al., 2001; Hinsinger et al., 2001; Dessert et al., 2003). Among different world regions, cold boreal zones have been studied only in Iceland (Gislason et al., 1996) and the Columbia Plateau (Dessert et al., 2003). Because of their small areas, these regions only weakly contribute to the overall continental basalt weathering and associated CO_2 consumption. Large boreal regions such as Central Siberia are likely to play a more important role because they offer extensive surface to weathering and they are overlaid by organic-rich permafrost soils and wetlands that constitute important carbon sink (Botch et al., 1995). Moreover, the behavior of chemical elements in the course of permafrost thawing and organic carbon mobilization induced by global warming are key environmental issues related to these regions (Guo et al., 2004). The increase of river discharge and the unfrozen layer thickness in the Russian Arctic over the past several decades (Peterson et al., 2002; Serreze et al., 2002; Oelke et al., 2003) have provoked the release of

* Author to whom correspondence should be addressed (oleg@lmtg.obs-mip.fr).

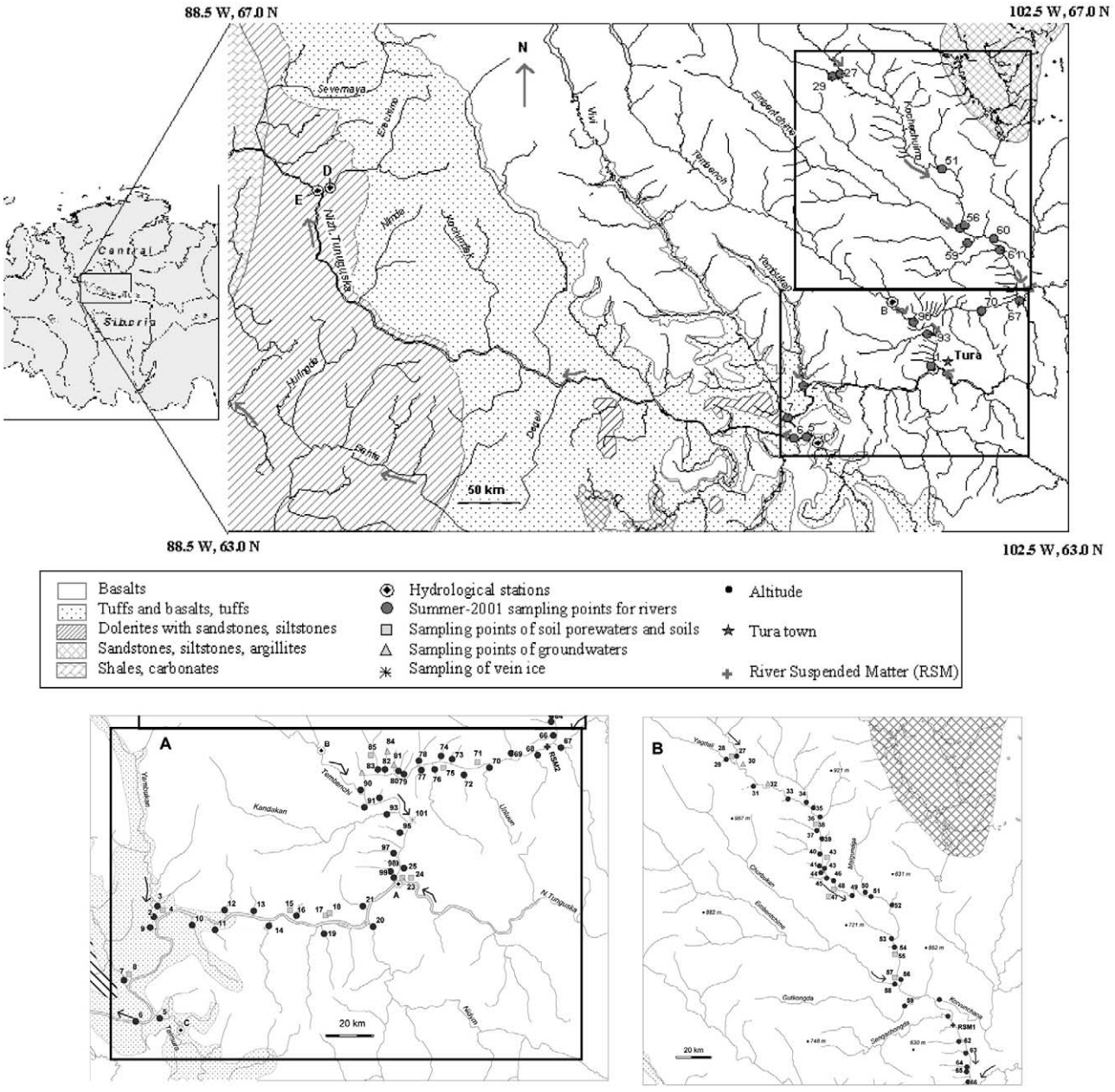

Fig. 1. Map of the area showing the rivers, hydrological stations, sampling points and geological situation. Sectors A and B.

carbon and metals trapped in the permafrost ice, which is likely to increase the fluxes of chemical elements to the ocean as well as to change their aqueous speciation and bioavailability. However, detailed studies of basalt weathering under boreal permafrost-dominated conditions are still lacking. To fill this gap, we have collected in the Nizhniya Tunguska river system (Yenisey Basin, Central Siberia, Fig. 1) over 100 samples of rivers, soil pore waters, and groundwaters, as well as soils, river suspended matter, and bed sediments. This region presents a unique opportunity for studying basalt weathering on a large scale because it combines homogeneously distributed soils and evenly developed vegetation over almost monolithologic terrains without any influence of industrial and agricultural activity (population density is less than 1 inhabitant/km^2), which allows us to consider that weathering occurs in a truly pristine area. Analyses of collected samples, combined with the long-term (1965–1975) data obtained from the Russian Hydrological Survey, provided a new picture of discharge and chemical composition of rivers draining monolithologic basaltic terrain, on short- and long-term scale. Building on this information and an original set of data, the purpose of this study is twofold. The first goal is a rigorous estimation of chemical elements and suspended matter fluxes for basaltic watersheds of various sizes and establishing the relative mobility of chemical elements during weathering. The second goal is to distinguish between the following possible sources of elements in river waters over the annual cycle and different seasons: fresh rocks, soils, vegetation litter and the permafrost ice, and underground reservoirs.

2. STUDIED AREA AND METHODS

2.1. General Setting of Putorana Basalts and the Territory Description

Traps of the Siberian Platform, covering an area of ~1,500,000 km^2 area with a total volume of 1,750,000 km^3, are located in the central and northern part of Siberia between the river Angora on the south and river Pyasina on the north, from the Yenissey on the west to middle river Vilyi on the east. The 248-Ma-old flood basalt complex covers a surface of 340,000 km^2 and forms a plateau with deep valleys; the highest elevations are 1500 to 1700 m. The thickness of individual lava flows varies between 20 and 40 m, and the overall thickness of lava formation in the central part of plateau is between 1500 and 2000 m, decreasing to 200 to 300 m in the southern part. In contrast to other basaltic provinces, Siberian traps exhibit a thick horizon of early Triassic tuff deposits (up to 700 m) formed before the massive lava eruptions. Despite some textural differences between different formations (i.e., Nidymskaya, Kochechumskaya, Yambukanskaya formations), Siberian basalts are very homogeneous in chemical and mineralogical compositions and are represented by tholeiites, typical for all trap formations of the world. Further geological, tectonic, and stratigraphic description of the territory can be found elsewhere (Lurie and Masaitis, 1958; Zolotukhin and Al'Mukhamedov, 1988; Courtillot and Renne, 2003).

The studied region belongs to the central and southern part of the basaltic province and includes all major tributaries of the river Nizhniya Tunguska (Fig. 1). Permafrost extends throughout the studied area; its thickness varies between 200 and 400 m. The temperature ranges between −3 and −8°C. The depth of the active (unfrozen) layer (June-August) ranges from 0.2 to 0.3 m on the northern slopes under clay soils, to 0.8 to 1.0 m on valley bottoms and slopes of southern exposition under sandy soils. The average annual soil temperature does not exceed 0°C.

The soils and vegetation of the region are quite homogeneous. Tundra dominates above 700 to 800 m, while open larch forest (*Larix gmelinii*) occurs at lower elevations (Abaimov et al., 1997). The soil types vary from lithosol, gelic gleysol, and regosol on the upper part of the plateau above 500 m, to gelic cambisol on the southern part of the plateau and the left tributaries of Nizhniya Tunguska (FAO/UNESCO, 1978). The upper 10-cm-thick organic-rich horizon is easily identifiable, but the other horizons are almost impossible to distinguish. On the ridges and plateau (200–400 m above the riverbed), the soil thickness does not exceed 10 to 20 cm. Most of tree roots are located in the upper 20- to 30-cm active layer. On well-drained areas, the roots reach the depth of 0.8 to 1.0 m (Abaimov et al., 1997). Loamy soil size distributions are very homogeneous with depth, typically, 10 ± 2% of 1 to 0.25 mm, 20 ± 4% of 0.25 to 0.05 mm, 30 ± 5% of 0.05 to 0.01 mm, 20 ± 4% of 0.01 to 0.001 mm and 20 ± 5% of <0.001 mm, as reported for several profiles on basalts and tuffs in the southern part of the Putorana Plateau (Sokolov, 1991).

The climate of the territory is continental, with a mean annual air temperature of −9 ± 1°C and variations from −37 (December) to + 17°C (July). The annual precipitation varies from 400 to 450 mm in the eastern part of the plateau to 500 to 550 mm in the western part, with 75% of precipitation occurring in August and September.

The annual pattern of river discharge exhibits very strong dependence on season and rain events (Fig. 2). Most annual discharge occurs during snow melt in May-June (60%–65%) and during summer rains (~30%). During the six winter months, from November to the end of April, the rivers carry only 5 to 10% of the annual discharge. During this time, concentration of dissolved elements in large rivers (Nizhniya Tunguska, Tembenchi) rises to 1 to 1.5 g/L (compared to 20–50 mg/L in summer), due to both weathering under low water/rock conditions and enrichment by salts (i.e., NaCl, $Ca(HCO_3)_2$, $MgSO_4$) originated from the deep/subsurface groundwaters formed by freezing concentration or associated with early Cambrian evaporates (Resources, 1973). The groundwater reservoir is relatively small; as a result, most of the small rivers are completely frozen for up to 180 days. Annual river runoff values for studied rivers vary from 200 mm (river Taimura N 5, Nidym N 20, Nizhniya Tunguska N 6) to 400 to 500 mm (rivers Tembenchi N 90, Yambukan N 2, Vivi N 7, Eratchimo (E), Kochechumo N 1). The highest runoff (600–800 mm/yr) is observed for the rivers draining the upper part of the Putorana Plateau (Yagdali N 29, Embènchimé N 58).

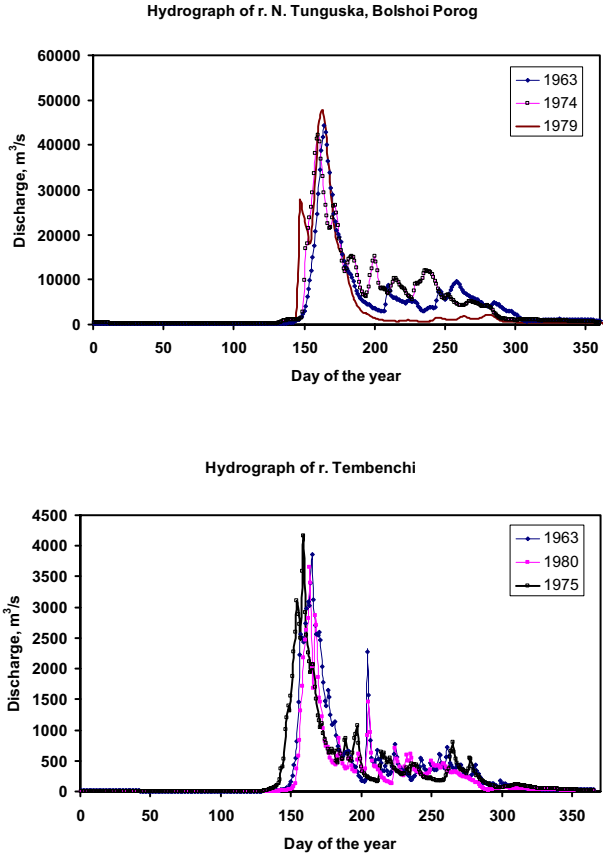

Fig. 2. Annual pattern of water discharge in the N. Tunguska River (D) and Tembenchi (B, N 90).

2.2. Sources of Information and Calculation Methods

Available data from systematic surveys by the Hydrometeorological State Committee of the former USSR Goskomgidromet and later Roskomgidromet, which were used to estimate the annual water and suspended and dissolved elements discharge for four rivers of the region as shown on the map (Fig. 1) by circled letters, are published in the annual issues of the State Water Cadastre (Hydrological Yearbooks, State Gidromet,1954–1975) and further generalized in *Resources of Surface Waters of the USSR, 1973*. The river watershed size varies from 9000 to 447,000 km^2. The data from the Hydrological Survey include, for each five hydrological stations (Nizhniya Tunguska at Tura [A], Nizhniya Tunguska at Bolshoi Porog [D], Tembenchi [B], Eratchimo [E], and Taimura [C]), the water daily discharge; from 4 to 11 measurements per year of major cations, anions, silica, iron, and organic carbon; and 15 to 30 measurements per year of total suspended matter (SM). Daily discharge values for all studied rivers were obtained from the stage-discharge rating curve established by the Hydrological Survey for each gauging station according to International Standards (International Organization for Standardization, 1983). Analyses of solutes and suspended matter performed by the Hydrological Survey are described elsewhere (Soyer and Semenov, 1971; Semenov, 1977; Gordeev and Sidorov, 1993; Zakharova et al., 2005).

Concentrations of calcium, magnesium, sodium and potassium, sulfate, bicarbonate, chloride, and total mineralization demonstrate a strong power dependence on water discharge. Because this dependence is valid over the full period of observations (1965–1975), it was used for the estimation of mean multiannual concentrations. For this pur-

pose, all chemical analysis data from 1965 to 1975 were used to generate the coefficients k and n in Eqn. 1:

$$C_i = k \cdot Q_i^n \quad (1)$$

where C_i represents measured ion concentration for a given day of the year, Q_i is water discharge for this day, k and n are empiric constants for each river. Examples of C versus Q dependence for some rivers and the values of k and n parameters are given in the Appendix 1 (Fig. A1-1–A1-5 and Table A1). For each gauging station, the value of mean annual water discharge available for the period of observations (Resources, 1973) was used to calculate the mean multiyear concentration of component i (Table A1) using Eqn. 1. A similar method was used for estimation of mean monthly and annual concentrations of elements in the rivers of Lena Basin (Gordeev and Sidorov, 1993) and the Transbaikal region (Zakharova et al., 2005).

The mean multiyear flux of element i (R_i) is calculated as

$$R_i = C_i^* \cdot W/A \quad (2)$$

where C_i^* is the mean multiyear concentration of element i calculated as described above and corrected for atmospheric input; A stands for the watershed area (km^2), and W is the multiyear average water discharge (km^3/yr) for the considered period, taken from the Hydrological Survey Database (Resources, 1973). The mean multiyear concentrations were corrected for atmospheric input by subtracting the average multiannual (each year in 1962–1985, and the year 1990) concentration of elements in the rain measured in the nearest meteorological station of the region (Turukhnask): [Mg] = 0.6, [Ca] = 0.5, [Na + K] = 1.15, [HCO_3] = 3.0, [SO_4] = 2.8, and [Cl] = 1.75 mg/L (Resources, 1973). The sea-salt normalized corrections, which use only Cl^- concentration in the precipitation according to Négrel et al. (1993), gave similar results within ±15% uncertainty. Note that the seasonal variations of atmospheric precipitates (by an order of magnitude) yield significant uncertainty on C_i^* value (i.e., 15%).

The annual SM fluxes were taken from the USSR Hydrological Survey database (Resources, 1973). The method of SM flux estimation used by the Hydrological Survey is based on the time interpolation between the values measured at the main phases of hydrological regime, and more frequently, at the rising water level (15–30 times per year).

2.3. Sampling and Analyses of Rivers and Soil Pore Waters

Field measurements included water temperature (±0.2°C) and pH (±0.02 U) of unfiltered samples. River water samples were collected from the beach, or with the rubber boat, near the middle of the flow; samples were collected in 1-L high-density polyethylene (HDPE) containers held on a nonmetallic stick. Plastic gloves were used during all manipulations. The collected waters were filtered through a 0.22 μm acetate cellulose membrane using a Sartorius polycarbonate filter holder and MITYVAC manual vacuum pump within 1 h after sampling. The first 200 to 400 mL of the filtrate were systematically discarded. Filtered samples were stored in acid-cleaned HDPE bottles, acidified to pH ~2 with bidistilled ultrapure HNO_3 for cations and traces, and nonacidified by HNO_3 for anions. Samples for dissolved organic carbon (DOC) were collected in pyrolyzed (550°C) Pyrex test tubes.

Aqueous silica concentration was determined colorimetrically (molybdate blue method) with an uncertainty of 2% using a Technicon automated analyzer. Alkalinity was measured by potentiometric titration with HCl to pH = 4.2 using a Gran method with a detection limit of 10^{-5} M and an uncertainty of 2%. DOC was analyzed using a carbon total analyzer (Shimadzu TOC 5000) with a detection limit of 0.1 mg/L and an uncertainty better than 3%. Organic carbon blanks of filtrates never exceeded 0.1 mg/L, which is quite low for the organic-rich rivers sampled in this study (i.e., 5–20 mg/L DOC). Major anion concentrations (Cl, SO_4, F, NO_3) were measured by ion chromatography (HPLC, Dionex 2000i) with a detection limit of 0.02 to 0.03 mg/L and an uncertainty of 2%. Calcium, magnesium, sodium, and potassium concentrations were determined using an atomic absorption Perkin Elmer 5100PC spectrometer with an uncertainty of 1 to 2%. The detection limits for measured cations were 1.4, 1.7, 1, and 6 μg/L for K, Na, Mg, and Ca, respectively. High concentrations of dissolved iron and aluminum (i.e., >0.5 mg/L) were measured by flame Atomic Absorption Spectroscopy (AAS), whereas the lower concentrations were analyzed by Inductively Coupled Plasma Mass Spectrometry (ICP-MS) (Elan 6000, Perkin Elmer). The international geostandard SLRS-4 (riverine water reference material certified by the National Research Council of Canada) was used to check the validity and reproducibility of the analyses. A good agreement between our replicated measurements of SLRS-4 and the certified values was obtained (relative difference <5%).

Soil pore waters were extracted from humid soil horizons in the field using a Ti pressure device. This titanium vessel has a 50 mm diameter, 150 mm length, and a special thread allowing it to reach 20,000 kg/cm^2 pressure. Depending on saturation state of soil samples, 10 to 50 mL of solution were collected. Extraction of soil pore water from the permafrost horizon was performed after sample thawing at ambient temperature (15 ± 5°C). Typically, 30 to 70 mL of interstitial water was collected from 1 L of frozen sample. After each extraction, the vessel and its compartments were thoroughly washed by river water, and afterward, by 100 to 200 mL of distilled water. Before and after fieldwork, blank samples were run by filling the pressure system with MilliQ water at neutral pH and letting it to react for 24 h. No detectable contamination of major and trace elements and DOC was observed. All soil pore waters analyzed in this work were filtered through a 0.22 μm acetate cellulose filter. Concentration of river suspended matter was determined by filtering large volumes (i.e., 1.5 to 3 L) of river water through a 0.22 μm acetate cellulose filter using a Sartorius polycarbonate filter holder. The filter was dried at 90°C during 48 h and weighted before use.

Groundwater samples were collected from the border of river valleys or canyons at the depth of 30 to 100 cm over the permafrost table. A sample of a ground ice vein (N 101) was collected from the depth of ~1.5 m on the Kochechumo valley slope just after its surface exposition following a solifluction event. This block of ice ~1 kg was melted at ~5°C during 2 h and the resulting solution was immediately filtered through 0.22 μm for chemical analyses.

2.4. Analysis of Solid Phases

Total chemical composition of rocks, sediments, and soils was performed after fusion of samples with $LiBO_2$, dissolution in HNO_3, and subsequent analysis by Inductively Coupled Plasma Atomic Emission Spectrometry (ICP-AES). Analyses of vegetation were performed after dissolving the dry, distilled-water rinsed biomass in HNO_3+ H_2O_2 during 24 h at 25°C and HF + HNO_3 digestion performed in the clean room on a hot plate at 60°C. Validity of total chemical analysis was verified by applying the same procedure for the International Standards BIR-1 of basalt, NIST 2711 of soil, and SRM 1515 of apple leaves tissue. Typical uncertainties on major element analyses were 1 to 2%. Altered and fresh rocks, and soil grain thin sections were analyzed with electron microprobe Camebax by the Wavelength Dispersive Spectrometry (WDS) technique using 15 KeV accelerating voltage. Clay fraction (i.e., <1 μm grain size) was separated by sedimentation in the water column. For structural X-ray diffraction analysis (XRD) performed on a DRON-4.0 apparatus, oriented samples were prepared by depositing a drop of <1 μm suspension on a glass plate and drying it at room temperature. Standard treatment in H_2O and ethylene glycol and heating at 550°C were employed to assess the interlayer distances of clay silicates following the technique developed on other mixed-layer minerals (Drits and Sakharov, 1976; Drits et al., 2002; Lindgren et al., 2002).

3. RESULTS

3.1. Characterization of Solid Phases

The total major chemical compositions of primary rocks (tuffs, basalts, dolerites), individual minerals, sampled soil horizons, riverbed sediments and suspended matter, and vegetation are given in Table 1. Based on results of ~130 optical microscope analysis, coupled with electron microprobe mea-

Table 1. Total chemical composition of solid samples, weight %. Ref. 1 = Ershov, 1994. I.L. = Ignition Lost.

Ref sample	fraction	C org	SiO_2	Al_2O_3	FeO	Fe_2O_3	Fe (total) as Fe_2O_3	MnO	MgO	CaO	Na_2O	K_2O	TiO_2	P_2O_5	I.L.	Total
SOILS:																
24, soil 40–50 cm	<1 μm		34.86	13.05			14.84	0.18	4.34	2.95	0.49	0.44	0.69	0.26	27.75	99.85
24, soil 40–50 cm	1–50 μm		40.86	14.09			12.21	0.2	4.32	5.85	1.41	0.45	1.21	0.21	18.46	99.27
24, soil 40–50 cm	<2 mm		45.57	14.17			11.38	0.19	5.56	9.48	1.87	0.37	1.34	0.17	9.74	99.84
26, soil 40–50 cm	<1 μm		35.51	12.2			16.55	0.18	4.76	2.71	0.49	0.38	0.8	0.25	26.06	99.89
26, soil 40–50 cm	1–50 μm		40.71	13.32			13.26	0.19	4.68	5.86	1.52	0.45	1.45	0.24	18.19	99.87
26, soil 40–50 cm	<2 mm		46.58	14.09			11.86	0.19	6.03	10.34	1.91	0.39	1.41	0.18	6.88	99.86
23, soil 20–40 cm	<1 μm		39.32	14.26			13.76	0.08	4.21	2.58	0.37	0.42	0.77	0.14	23.93	99.84
23, soil 20–40 cm	1–50 μm		43.88	14.78			11.49	0.15	4.36	5.49	1.45	0.55	1.25	0.15	16.3	99.85
46, soil 8–10 cm	<1 μm		38.01	15.26			14.76	0.14	4.12	2.52	0.38	0.57	0.71	0.28	23.17	99.92
46, soil 8–10 cm	1–50 μm		46.23	15.97			11.98	0.19	4.47	6.89	1.82	0.62	1.52	0.2	9.97	99.86
47, soil 8–12 cm	<1 μm		22.63	15.00			14.26	0.04	1.12	0.91	0.32	0.26	0.57	0.6	44.5	100.21
47, 8–12 cm	1–50 μm		34.69	15.95			12.11	0.07	2.24	2.47	1.04	0.38	1.13	0.36	29.38	99.82
47, soil 8–12 cm	<2 mm		34.49	14.11			12.83	0.11	3.78	4.39	0.94	0.33	1.43	0.31	27.13	99.85
38, soil 10–20 cm	<1 μm		35.27	10.81			20.4	0.15	6.28	2.93	0.65	0.35	0.63	0.23	22.17	99.87
38, soil 10–20 cm	1–50 μm		46.40	16.13			12.34	0.18	5.47	9.41	2.31	0.36	1.65	0.18	5.43	99.86
38, soil 10–20 cm	<2 mm		45.80	14.28			11.74	0.19	6.14	10.15	1.93	0.31	1.33	0.16	7.81	99.84
28a, soil 20–30 cm	<1 μm		33.39	12.83			16.17	0.28	5.55	3.3	0.64	0.42	0.68	0.48	25.81	99.55
28a, soil 20–30 cm	1–50 μm		41.35	15.52			13.11	0.23	5.05	6.81	1.69	0.33	1.23	0.21	14.33	99.86
28a, soil 20–30 cm	<2 mm		46.15	14.20			12.78	0.23	6.45	10.51	1.99	0.3	1.46	0.17	6.16	100.4
8, soil 50–60 cm	<2 mm		48.12	15.36			10.88	0.16	4.71	7.03	2.02	0.62	1.16	0.13	9.68	99.87
17b, soil 5–15 cm	<2 mm		42.02	14.47			10.77	0.14	4.36	6.94	1.61	0.49	1.13	0.18	17.72	99.83
17a, soil 80–90 cm	<2 mm		43.02	13.77			11.45	0.16	4.68	7.43	1.58	0.47	1.23	0.18	15.88	99.85
18c, soil 50 cm	<2 mm		45.20	14.98			13.52	0.23	5.46	9.23	1.75	0.14	1.55	0.16	8.01	100.23
48a, soil 0–10 cm	<2 mm		23.16	7.11			5.86	0.08	2.57	5.44	0.9	0.13	0.66	0.14	54.17	100.22
48b, soil 10–20 cm	<2 mm		41.8	15.26			11.15	0.21	3.95	5.96	1.32	0.45	1.31	0.13	18.3	99.84
55, soil 20 cm	<2 mm		43.28	15.52			12.97	0.16	4.84	6.52	1.4	0.39	1.68	0.13	12.47	99.36
71b, soil 10–20 cm	<2 mm		47.14	15.14			11.91	0.2	5.37	9.04	1.84	0.43	1.39	0.16	7.24	99.86
89, soil 30–50 cm	<2 mm		47.48	10.27			13.87	0.25	8.71	12.82	1.41	0.23	2.34	0.15	2.47	100
River Suspended Matter (RSM):																
RSM-1	<2 mm	0,48	46.77	15.05			11.19	0.18	5.84	10	2.14	0.33	1.3	0.15	5.78	98.73
RSM-2	<2 mm	0,38	47.77	15.16			11.6	0.19	6.09	10.58	2.1	0.32	1.35	0.15	4.16	99.47

River Bed Sediments (RBS)

Ref sample	fraction	SiO_2	Al_2O_3	FeO	Fe_2O_3	Fe (total) as Fe_2O_3	MnO	MgO	CaO	Na_2O	K_2O	TiO_2	P_2O_5	I.L.	Total
53, RBS	<1 μm	36.91	11.83			17.18	0.19	6.45	3.84	0.6	0.48	0.65	0.29	22.05	100.47
53, RBS	1–50 μm	43.55	14.69			14.2	0.25	5.38	6.64	1.72	0.5	1.49	0.24	11.82	100.48
33, RBS	1–50 μm	44.75	16.83			13.11	0.29	4.63	8	2.12	0.39	1.36	0.22	8.16	99.86
33, RBS	<2 mm	47.79	14.7			12.4	0.23	6.48	11.36	2.14	0.33	1.32	0.18	3.21	100.14

Table 1. (Continued)

Ref sample	fraction	SiO_2	Al_2O_3	FeO	Fe_2O_3	Fe (total) as Fe_2O_3	MnO	MgO	CaO	Na_2O	K_2O	TiO_2	P_2O_5	I.L.	Total
River Bed Sediments (RBS)															
10, RBS	<2 mm	48.18	13.75			12.16	0.22	5.59	8.29	2	0.66	1.3	0.17	7.68	100
21, RBS	<2 mm	46.7	15.24			12.57	0.22	5.96	10.04	2.09	0.28	1.42	0.18	5.16	99.86
19, RBS	<2 mm	51.99	13.77			11.26	0.21	5.38	8.81	2.02	0.71	1.27	0.17	4.28	99.87
5, RBS	<2 mm	53.18	14.43			8.82	0.16	4.04	5.11	2.39	1.21	1	0.15	9.91	100.4
13, RBS	<2 mm	49.84	13.68			12.0	0.22	6.01	10.39	2.09	0.44	1.37	0.17	3.66	99.87
20, RBS	<2 mm	48.69	15.41			10.76	0.15	4.75	7.44	2.13	0.68	1.18	0.15	8.57	99.91
7, RBS	<2 mm	47.65	14.35			11.49	0.18	6.01	9.53	2.1	0.45	1.28	0.16	6.7	99.9
2, RBS	<2 mm	46.46	14.79			11.88	0.17	5.68	8.4	2.29	0.5	1.24	0.18	8.88	100.47
6, RBS	<2 mm	56.15	13.86			8.48	0.13	3.98	5.42	2.46	1.34	0.93	0.13	7.01	99.89
Vegetation:															
Larch litter, *Larix gmelinii*		3.91	1.09			0.729	0.073	0.584	1.32	0.122	0.388	0.105			
Green Moss, *Hylocomium s.*			0.055			0.055	0.05	0.158	0.382	0.032	0.074	0.0058			
Lichens *Cladonia s.*			0.02			0.014	0.01	0.027	0.054	0.016		0.0017			
PARENT ROCKS:															
Dolerites, Tembenchi	bulk	48.52	15.05	10.23	2.28		0.25	7.4	10.63	2.21	0.46	1.64	0,14	0.74	99,55
Trappes (av. 179), Ref. 1	bulk	48.3	15.5	9.4	3.6		0.2	6.2	10.7	2.2	0.7	1.5	0,1		
Tuffs (av. 10), Ref. 1	bulk	55.5 ± 3.5	14.6 ± 1.1		8.5 ± 3.5		0.15 ± 0.05	3.0 ± 1.0	7.0 ± 3.0	1.45 ± 0.05	0.80 ± 0.45	1.2 ± 0.5	0,1		
MINERALS (EMA of thin sections of basalts from Tembenchi and Kochechumo rivers)															
Interstitial glass		42.3 ± 2.6	7.7 ± 0.8	23.9 ± 3.9			0.16 ± 0.1	9.1 ± 4.1	3.2 ± 1.9	0.84 ± 0.8	0.32 ± 0.2	0.57 ± 0.5			
Smectite post-olivine (I)		40.7 ± 3.9	5.3 ± 0.6	24.1 ± 0.9			0.1 ± 0.03	12.0 ± 1.4	2.3 ± 0.3	0.4 ± 0.3	0.3 ± 0.25	0.1 ± 0.03			
Clays developed on interstitial glass (II)		45.5	5.2	19.8			0.05	15.8	1.4	0.15	0.20	0.07			
Plagioclases (av. 20) analyses)		51.4 ± 1.4	29.6 ± 1.1	0.96 ± 0.3				0.04 ± 0.03	13.7 ± 1.2	3.84 ± 0.63	0.24 ± 0.2	0.037 ± 0.025			
Pyroxenes (av. 10 analyses)		50.2 ± 1.1	1.95 ± 0.6	13.8 ± 4.6			0.35 ± 0.1	14.3 ± 1.9	17.8 ± 3.1	0.15 ± 0.09	0.01 ± 0.005	1.0 ± 0.4			
Titano-magnetite		0.06	0.08	37.3			0.53	0.46	0.09	0.0004	0.009	54.8			

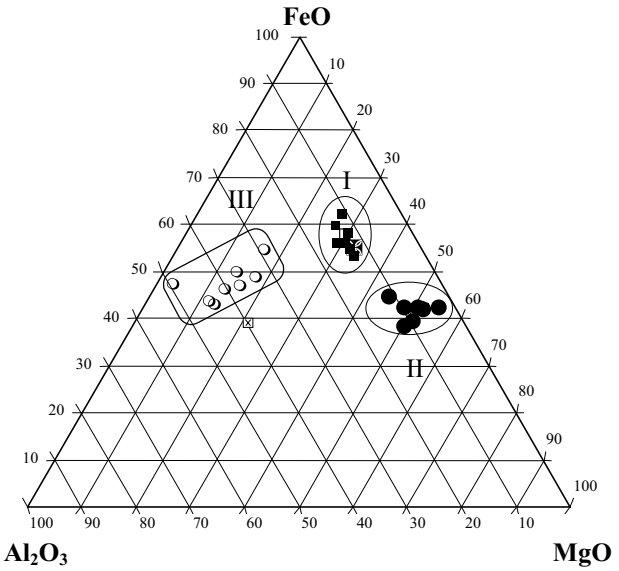

Fig. 3. Ternary diagram of smectite composition. I group (solid squares), post-olivine smectite (samples 55, 47); II group (solid circles), interstitial smectite 1 μm fraction of soil samples 23, 24, 26, 48, 28a and RBS 53). Individual symbols stand for ⊠, basalt (this study); ⊞, oxy-smectite (Dainyak et al., 1982).

surements on thin sections of fresh basalts sampled over r. Tembenchi (B, No 90) and right tributaries of river Nizhniya Tunguska, we estimated the volume proportions of major rock-forming minerals: 25 to 30% of pyroxene (augite), 40 to 45% of plagioclase An_{55-60}, 5 to 10% of interstitial glass and 20 to 25% of clays (essentially trioctahedric smectite with d_{060} = 1.536 Å). The chemical composition of plagioclases, pyroxenes, interstitial glass, and smectite, assessed from electron microprobe analysis of thin sections of basalt collected over Tembenchi and Kochechumo river basins, is presented in Table 1. In tuffs, the proportion of interstitial glass increases to 20 to 30%, and the anorthite content in plagioclase decreases to An_{40-50}.

In thin, 1 to 2 mm, weathering rings of basalts investigated by electron microprobe analysis (EMA) in both altered rocks and sediments, the interstitial basaltic glass is often transformed into an amorphous Fe-Al rich phase. This is consistent with previous observations in this region showing that the accumulation of secondary Fe and Al phases in soils occurs in the form of amorphous metal humates and allophanes (Samoilov, 1989; Sokolov, 1991).

Among the clays, dioctahedral smectite (d_{060} = 1.52 Å) representing pseudomorphoses on glass, accounts for only 1 to 3% of glass (i.e., <1% of total rock volume). Three major groups of smectites can be identified based on electron microprobe analysis of thin sections (Fig. 3). The first group, encountered in fresh rocks, is represented by iron-rich postolivine smectite and oxy-smectite (Fe^{3+}- trioctahedric 14.80 Å smectite; Kudryavtzev, 1979; Dainyak et al., 1982). Transformation of this trioctahedral oxy-smectite into dioctahedral smectite was occasionally observed on the weathering rings at the mineral surfaces. Smectites of the second group replace the interstitial glass, and compared to those of the first group, they are enriched in Mg. Finally, smectite from the river alluvium and soils (<1 μm fraction) is depleted in Mg and enriched in Al, thus confirming the relative order of element mobility during weathering.

Alluvium formed during basalt degradation is represented by fractions from 0.05 to 2 mm. The dominant fraction of riverbed sediments for Tembenchi and Kochechumo, 0.125 to 0.63 mm, accounts for ~90% of sand. The mineralogical composition of river alluvium is different from that of fresh rock with an enrichment in pyroxenes and a strong depletion in smectite, which are transported as river suspended matter (Fig. 4a).

Mineral composition of solid material was further characterized by structural X-ray analyses of fine (<0.001 mm) and bulk fractions of two samples of river sediments (samples 33 and 53) and eight samples of soils (samples 18c, 23, 24, 26, 28a, 38, 47, and 89). Regardless of sample location over the territory and

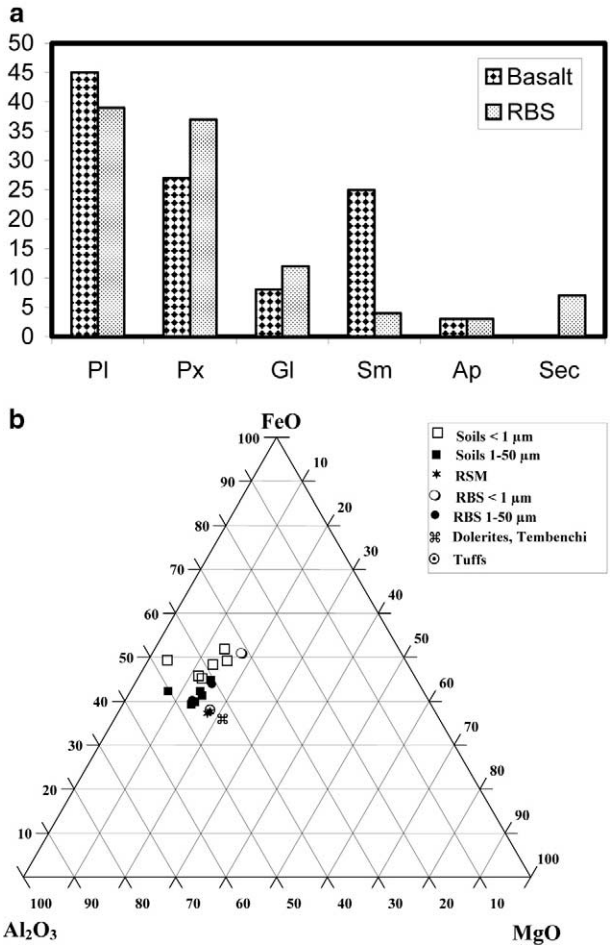

Fig. 4. (a) Mineralogical composition of fresh basalt and river alluvium (RBS) collected on rivers Tembenchi and Kochechumo based on average of 35 (basalt) and 20 (alluvium) samples. P1 = plagioclases (An_{55-60} in basalts, An_{40-50} in sands); Px = pyroxenes (99% augite, ~1% pygonite); Gl = volcanic glass (in RBS, partially altered and covered by Fe oxy(hydr)oxides); Sm = smectite; Ap = heavy ore minerals (Ti-magnetite); Sec = secondary minerals (quartz, zeolites, prenite). (b) Chemical differentiation between fresh rocks (dolerites, tuffs), soils, river alluvium and river suspended matter. Sand fraction (1–50 μm) of both soil and sediments is enriched in Al because of presence of plagioclase grains, and magnesium is removed during transformation of basalts to soil and river sediments.

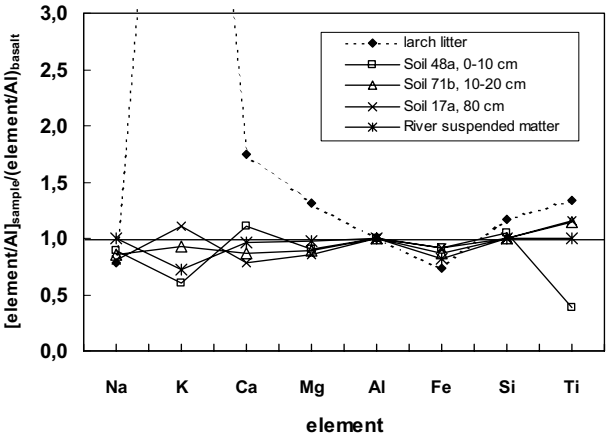

Fig. 5. Aluminum-normalized elemental ratios in plant litter, soils and river suspended matter compared to the initial rock (traps). Strong enrichment of plant litter by potassium (factor 8) is out of the scale.

type of solid material (i.e., riverbed sediments or various soil horizons), all fine fractions exhibit the presence of mixed-layer illite-smectite (20 ± 10% of illite layers) as secondary phases, and traces of chlorite, quartz, feldspars, and, sometimes calcite (the latter is only in samples 28a and 47). This is consistent with previous studies of Putorana soils; according to Sokolov and Gradusov (1978) and Gradusov and Ivanov (1983), chlorite-smectite (10–15 Å) with trioctahedral smectite and chlorite (14 Å) are the dominant minerals in <1 μm fraction, with some proportion of amorphous compounds such as allophanes.

The chemical composition of soils and sediments and river suspended matter is compared in an Al-Fe-Mg ternary diagram (Fig. 4b). The sand fraction (1–50 μm) of both soil and sediments is enriched in Al because of the presence of plagioclase grains and the depletion of magnesium, which is removed during basalt weathering. No major differences can be detected between soil horizons, sediments of different rivers of the territory, and river suspended matter. As expected, these solid phases are depleted in Mg and enriched in Fe compared to fresh rocks. In accord with numerous studies of soils in the Siberian traps region (Sokolov and Gradusov, 1978; Sokolov and Bystryakov, 1980; Gradusov and Ivanov, 1983; Sokolov, 1991; Ershov, 1994; Ershov, 1995), the chemical composition changes only weakly with depth of soil (i.e., compare samples 17a and 17b, 23 and 24). Over the area of more than 90,000 km^2 investigated in the present study, the chemical composition of soil stays constant, as assessed from the comparison of samples 26, 28 (the most northern part), and 8, 55, and 89 (southern and central part). Sample 38, which represents a typical gley soil developed on the periodically flooded river bank, has the highest Fe content among all studied soils.

Another important "solid" reservoir of chemical elements is plant litter and grass biomass. Expressing concentrations in weight % of dry biomass, it appears that the larch litter is 4 to 7 times depleted in Ca, 5 to 10 times in Mg, 10 to 13 times in Si, Fe, Al, and Ti, compared to river suspended matter and the deep soil horizons. Assuming aluminum is mostly immobile during weathering (Polynov, 1944; Chesworth et al., 1981), one can compare the aluminum-normalized elemental ratios in "secondary" solid reservoirs with those in basalt (Fig. 5). Compared to all inorganic pools, the larch litter is strongly enriched in Ca (by a factor of 1.7) and K (by a factor of 8, not shown). For other elements, in accord with previous discussion, no significant differentiation between rocks, river alluvium and suspended river matter, soil upper horizon, and larch litter is observed.

3.2. Hydrochemistry

Concentrations of major elements vary by a factor of 10 to 100 over the annual cycle, exhibiting a power dependence on the discharge. The 1965 to 1975 data of the Hydrological Survey (HS) are illustrated for rivers Nizhniya Tunguska (A, E), Eratchimo (D), Taimura (C), and Tembenchi (B) in Appendix 1 (Fig. A1-1 to A1-5). The chemical composition of rivers, and soil pore waters and groundwaters, sampled in 2001 is given in Tables 2 and 3, respectively. The average annual and summer period concentrations of dissolved components extracted from the HS database for rivers Tembenchi, Taimura, and Nizhniya Tunguska agree with our field data of July and August 2001 within 30 to 50%. This allowed us to use our summer 2001 concentration values for approximating the average annual concentrations and calculating element fluxes for other rivers of the territory. For most rivers, the total concentration of dissolved solids ranges from 30 to 70 mg/L, and calcium and sodium dominate among cations. The normalized inorganic charge balance (NICB $= \Sigma^+ - \Sigma^-)/\Sigma^+$) calculated for all studied rivers is 0.13. Only the organic-rich rivers having [DOC] $>$ 20 mg/L exhibit an important nonbalanced anion deficit ($0.2 \leq$ NICB ≤ 0.7), which is typical of boreal waters (i.e., Pokrovsky and Schott, 2002). Taking account of carboxylic group concentration in humic acids (10 μeq COO^- per mg DOC; Oliver et al., 1983) yields an average unbalanced charge of 0.04. Our ultrafiltration experiments (Pokrovsky et al., 2005c) demonstrated that only a small part of cations such as Ca or Mg (i.e., less than 10%) is associated with organic colloids (1 kD–0.22 μm). Therefore, although DOC is an important component for charge balance in solution, its overall role on alkali and alkali-earth element speciation is low, and Ca/Mg-organic complexes do not contribute more than 10% to the overall fluxes. Generally, the chemical composition of Putorana rivers is similar to that of other basaltic regions of the world; mean multiannual [HCO_3^-] (34 ± 9 mg/L) and [Na + K] + [Ca] + [Mg] (27 ± 7 mg/L) for four Siberian rivers are very close to the world average (33 and 21 mg/L, respectively, as calculated for the 12 most representative basaltic provinces; Dessert et al., 2003).

3.2.1. *Dissolved and suspended matter fluxes*

The average multiannual total dissolved solid (TDS) cation flux corrected for atmospheric precipitation of the studied rivers (TDS_c = Ca + Mg + Na + K) varies from 5 to 7 t/km^2/yr for rivers Taimura, Tembenchi, and Nizhniya Tunguska, to 19 t/km^2 for Eratchimo River (Table 4). Calcium and sodium dominate the cationic flux, accounting for 80% of TDS_c value. The majority of cations are released during the spring flood (June). The middle water season (July–October) yields 30 to 40% of the annual flux and the glacial season (November to April) accounts for less than 10%, as illustrated for river

Table 2. Chemical composition of rivers (<0.22 μm), SM = suspended matter, N.D. = non determined.

Number	Sample description	T, °C	SM mg/L	pH	DOC μM	HCO_3 μM	Cl μM	SO_4 μM	Si μM	Na μM	K μM	Mg μM	Ca μM	Al μM	Fe μM
N 1	r. Kochechumo before rains	18	29	7.51	758	407	218	7.1	193	139	12.8	78	194	1.6	1.7
N 2	r. Yambukan	14	70	7.49	1117	430	493	13.3	232	183	5.1	82	310	3.0	2.7
N 5	r. Taimura	15	2.1	7.63	1350	997	639	139.8	211	783	7.7	148	397	2.0	2.8
N 6	r. N. Tunguska	16.5	14	7.70	667	592	755	34.7	196	743	10.3	111	236	1.4	2.0
N 7	r. Vivi	14.5	5	7.75	592	511	444	20.4	189	417	2.6	78	231	1.5	1.9
N 10	r. Khenochangda	11.5	<1	7.60	1600	449	282	10.2	261	339	7.7	70	231	4.9	2.5
N 11	r. Dikkit Left	15	<1	7.77	1217	656	194	22.4	254	470	2.6	115	218	2.8	2.1
N 12	r. Delindeken (right)	15	<1	7.59	1208	539	20	12.2	254	200	2.6	82	174	3.5	2.0
N 13	r. Degigli (right)	13.5	<0.1	7.63	1108	589	183	14.3	261	396	2.6	107	226	2.6	1.8
N 14	r. Chunchan (left)	16	<0.1	8.00	1000	911	122	74.5	250	548	5.1	103	315	1.1	1.5
N 16	r. Goncha	12.5	<0.1	7.74	758	761	23	31.6	250	448	2.6	82	132	1.1	1.0
N 19	r. Ganalchik (left)	15.5	<0.1	7.82	1058	754	621	14.3	261	761	5.1	99	340	1.1	1.7
N 20	r. Nidym	19	<0.1	7.84	850	930	2194	48.0	221	791	15.4	152	950	0.5	2.5
N 21	r. Dilingda	14	<1	7.65	1867	575	9	4.1	254	126	2.6	103	196	1.7	1.4
N 22	r. Kochechumo near Tura	15.5	<1	7.70	2892	470	250	6.1	196	187	2.6	82	206	1.1	1.4
N 25	r. Kulingdakan	19	<1	7.67	1000	734	3	0.0	300	139	2.6	111	236	1.3	1.6
N 27	r. Kochechumo above Yagdali	16.5	0.25	7.49	375	444	253	6.1	193	165	2.6	86	203	1.0	1.2
N 29	r. Yagdali	17.5	1.0	7.90	233	526	145	12.2	175	126	2.6	95	211	0.4	0.9
N 33	r. Krivoruchka (right)	13	N.D.	7.30	650	323	3	5.1	175	57	2.6	66	89	N.D.	N.D.
N 34	r. Anakit (left)	18	N.D.	7.55	667	444	189	13.3	232	217	2.6	107	186	1.1	1.2
N 35	r. Vosgen (left)	16.5	N.D.	7.53	933	438	3	3.1	254	78	2.6	86	122	2.7	1.5
N 36	r. Anakit Low (left)	17	N.D	7.56	675	500	75	13.3	232	152	2.6	82	216	N.D.	N.D.
N 37	r. Gukdakan	15	N.D.	7.30	542	444	3	5.1	204	78	5.1	86	146	1.4	1.1
N 39	r. Mundakit Left	13	N.D.	7.54	767	407	3	3.1	186	61	5.1	99	124	N.D.	N.D.
N 40	r. Khunktukun	14.5	N.D.	7.65	733	544	3	3.1	239	96	2.6	107	156	N.D.	N.D.
N 41	r. Manashveika from swamp	14.5	N.D.	7.56	775	426	3	0.0	189	78	2.6	95	112	N.D.	N.D.
N 43	r. Yakovkhan after 15 hrs rain	12	N.D.	7.52	833	557	3	1.0	204	78	2.6	132	164	1.7	1.8
N 44	r. Ankatakan	11.5	N.D.	7.63	908	561	3	0.0	229	100	2.6	119	174	1.9	2.0
N 45	r. Vaskinkhan rising level	9.5	10	7.34	1142	330	0	0.0	218	70	2.6	74	92	4.4	2.5
N 46	r. Kochechumo on rising level	12	13	7.59	650	457	250	9.2	204	187	5.1	99	199	1.0	1.1
N 49	r. Kochechumo on max level	8.5	95	7.48	1492	393	81	8.2	200	104	5.1	78	146	N.D.	N.D.
N 50	r. Maigungda low max level	8.5	N.D.	7.55	1475	380	3	0.0	200	70	2.6	95	104	2.3	1.7
N 51	r. Kochechumo on decreasing level	8.5	N.D.	7.53	692	393	46	8.2	193	91	10.3	78	132	N.D.	N.D.
N 52	r. Khungtukun (left)	8	N.D.	7.41	4000	451	58	6.1	N.D.	74	2.6	99	114	2.4	2.2
N 53	r. Dalgakan (right)	8	N.D.	7.23	1175	307	3	2.0	243	78	2.6	74	99	3.7	2.1
N 56	r. Kochechumo	N.D.	14	N.D.	650	392	55	6.1	214	91	2.6	70	114	1.5	1.4
N 58	r. Embéntchimé	12	10	7.55	875	479	119	6.1	229	148	2.6	156	154	1.9	2.3
N 59	r. Gutkongda (right)	10.5	17	7.34	1350	367	12	0.0	225	83	2.6	86	109	2.1	1.3
N 60	r. Korvunchana	10.5	0.1	7.36	1058	356	46	6.1	225	100	2.6	74	104	1.7	1.5
N 61	r. Sengachangda	10	5.0	7.39	2158	448	67	3.1	257	117	2.6	91	181	1.9	1.2
N 62	r. Itchon	8.5	N.D.	7.16	1250	307	3	3.1	250	61	2.6	74	109	3.9	2.5
N 63	r. Degdutche	9	N.D.	7.31	1308	403	0	0.0	246	78	5.1	86	141	2.8	2.2
N 64	r. Delimekit High	8.5	N.D.	7.51	908	685	67	1.0	271	126	2.6	128	213	N.D.	N.D.
N 65	r. Delimekit	8.5	N.D.	7.21	1333	323	9	3.1	257	70	2.6	70	112	3.3	2.1
N 66	r. Delimekit Low	8	N.D.	6.99	1150	402	0	5.1	261	78	0.0	78	166	N.D.	N.D.
N 67	r. Turu	11.5	<0.7	7.04	1333	403	84	3.1	246	100	2.6	82	179	2.0	1.9
N 68	r. Inagli	12	<0.1	6.93	1700	392	15	11.2	261	83	2.6	82	166	3.0	1.3
N 69	r. Khokogangan	11	N.D.	7.06	1225	402	0	4.1	257	78	2.6	82	134	4.4	2.4
N 70	r. Untuun	10.5	N.D.	7.38	1300	698	148	4.1	268	200	5.1	111	266	1.6	2.9
N 72	r. Solokit	12	N.D.	7.41	1183	649	6	4.1	250	104	2.6	99	340	N.D.	N.D.
N 73	r. Uredy	11.5	N.D.	7.40	1442	479	3	2.0	293	78	0.0	95	194	3.0	2.5
N 74	r. Ugedy	10	N.D.	7.31	1508	403	3	3.1	264	65	0.0	82	169	4.6	2.8
N 76	r. Yukteli	16.5	N.D.	7.72	1800	625	107	16.3	279	226	7.7	95	266	2.1	2.5
N 77	r. Lyalyukta	12	N.D.	7.55	1308	490	3	3.1	279	91	2.6	86	184	N.D.	N.D.
N 78	r. Mosady	9	N.D.	7.43	1100	452	3	2.0	268	87	0.0	86	124	N.D.	N.D.
N 79	r. Vos'merka	8.5	N.D.	7.24	1492	339	3	4.1	304	87	0.0	66	114	5.9	3.4
N 80	r. Mutnyi	13	23	7.87	1267	739	3	0.0	325	165	5.1	111	211	N.D.	N.D.
N 82	r. Tutoka	16	<2	7.79	1142	625	3	1.0	282	126	5.1	115	196	2.0	2.3
N 83	r. Munasrakit before rain, discharge 0.5 m^3/s	12.5	2.0	7.75	1075	716	3	2.0	307	174	5.1	136	206	1.2	1.5
N 86	r. Munasrakit after 2 hrs rain, discharge 2.0 m^3/s	12	27	7.67	1017	744	3	4.1	296	183	2.6	128	208	1.0	0.9
N 87	r. Munasrakit after 12 hrs rain, discharge 5.0 m^3/s	10.5	61	7.23	1500	430	3	3.1	264	139	5.1	86	124	2.4	2.2
N 90	r. Tembenchi	15.5	11.5	7.51	900	566	171	9.2	214	235	2.6	86	213	1.4	1.6
N 91	r. Culkan	11.5	45	7.46	1833	549	0	4.1	314	143	2.6	99	243	2.4	2.0
N 93	r. Kandakan	14	25.5	7.57	1200	490	35	8.2	336	187	2.6	82	179	1.6	1.4
N 95	r. Vaskinkhan	9		7.61	1792	661	1	2.8	325	148	5.1	103	233	2.3	3.1
N 96	r. Kochechumo above Tura, (> 3 m water level increase)	9	155	7.39	13.5	1125	452	93	5.1	225	148	2.6	91	0.9	0.9
N 97	r. Anmundakit (right)	9	N.D.	7.31	1600	469	3	2.0	318	117	5.1	82	174	4.2	3.0
N 98	r. Svetlyi (right)	11	29	7.57	1158	697	26	6.1	325	170	2.6	99	248	1.6	2.0
N 99	r. Gremuchyi	10	35	7.63	1583	480	3	2.0	289	117	5.1	78	174	3.4	2.4
N 100	r. Kulingdakan	11	117	7.63	2142	575	6	4.1	296	130	2.6	99	201	2.4	2.8
	Average of 70 rivers	12	N.D.	7.51	1250	525	125	9.8	246	187	3.6	95	196	2.0	1.8

Table 2. (Continued)

Number	Sample description	T, °C	SM mg/L	pH	DOC μM	HCO_3 μM	Cl μM	SO_4 μM	Si μM	Na μM	K μM	Mg μM	Ca μM	Al μM	Fe μM
						Rains:									
	Rain on 26-07-01	17	N.D.	5.20	25	N.D.	73	0.00	0	1.0	2.0	0.5	0.7	4.2	3.0
	Rain on 10-08-01	14	N.D.	4.95	36	7	2	0.00	0	1.7	2.5	0.9	2.2	3.4	2.4
	Rain on 16-08-01	16	N.D.	4.23	N.D.	2	11	10.82	0	11.4	8.5	1.7	4.5	0.0	0.0
	Rain on 23-08-01	12	N.D.	5.37	N.D.	3	2	1.04	0	2.0	1.6	0.9	2.0	0.0	0.0

Tembenchi in Figure 6. These seasonal features of flux distribution are similar to those reported for granitic rivers from the Aldan Shield (Zakharova et al., 2005).

The concentration of dissolved organic carbon in ~60 large and small rivers sampled in 2001 varies between 7 and 20 mg/L, with an average of 14 mg/L. The most northern rivers issued from the upper part of the Putorana Plateau such as Yagdali (N 29) and Kochechumo (N 27) exhibit the lowest [DOC], while the rivers originated from swamp zones (Khenochangda N 10, Sengachangda N 61, Korvunchana N 60) exhibit higher [DOC] values. According to the measurements of the Hydrological Survey, the organic carbon concentration is quasi-constant during high and medium water seasons (discharge >1000 m^3/s, June–September) and close to the discharge-weighted average annual values (Fig A2, Appendix 2). These relations allow us to use the summer 2001 values of [DOC] measured for rivers Tembenchi, Taimura, and Nizhniya Tunguska to calculate the mean annual flux of organic carbon for the territory (Table 4). For all rivers, the flux of organic carbon in the form of DOC is 1.5 to 2 times higher than that of inorganic carbon in the form of HCO_3^-.

Suspended matter concentration varies between 50 and 100 mg/L during the spring flood and summer rain events, and 1 to 10 mg/L during the low water seasons, and correlates with the discharge. For rivers Eratchimo and Taimura, mean multiannual (1976–1979) SM concentrations were calculated to be 12 mg/L (Eratchimo) and 17 mg/L (Taimura). Our results collected in 2001, both at low water stage (samples 1–40, 25 July–8 August) and during the summer rain flooding (samples 41–100, 9 August–26 August) for 27 small and large rivers, are in agreement with these values. For rivers Taimura and Eratchimo, it was possible to make reliable estimates of annual SM flux because sufficient mean monthly data from the Hydrological Survey were available. The SM flux ranges from 3.1 ± 0.5 t/km^2/yr for r. Taimura to 9.0 ± 1.5 t/km^2/yr for r. Eratchimo. Using these data, we estimated the relative proportions of suspended and dissolved (<0.22 μm) fluxes for Na + K, Ca, Mg, Si, Fe, Al, Mn, and Ti in r. Taimura (Fig. 7). The following assumptions have been made for these calculations: (i) the chemical composition of suspended load does not vary significantly among the rivers of the region; therefore, the chemical composition of r. Kochechumo suspended load collected during summer rain flooding (samples RSM-1 and RSM-2) is equivalent to that of r. Taimura (point C in Fig. 1); (ii) summer 2001 concentrations of dissolved trace elements (Mn, Fe, Al, and Ti) and organic carbon in the r. Taimura are close to the average annual values (this condition is met for major elements). It can be seen in Figure 7 that a typical order of element mobilities in surface waters during rock weathering is observed: Na, K > Ca > Mg > Si > Fe ≥ Mn ≥ Ti ≥ Al (Polynov, 1944). This row should not be affected by the presence of halite and other evaporate minerals in the basin (see section 4.1). The relative order of mobility among Fe, Mn, Al, and Ti may be affected by different contributions of colloidal forms, since, except for Mn, the proportion of Al, Fe, and Ti in <1 kD pool is less than 1 to 10% (Pokrovsky et al., 2005c). The proportion of organic and inorganic carbon in the solid phases is negligible compared to that in dissolved form. This is typical for many Arctic rivers, such as N. Dvina, Pechora, Ob, and Lena, for which the dissolved/particulate organic carbon ratio (DOC/POC) varies from 6 to 40 (Gordeev et al., 1996).

3.2.2. *Composition of soil pore waters and groundwaters*

Chemical composition of soil pore waters and groundwaters sampled in July–August 2001 is given in Table 3. Throughout the studied territory, soil pore waters, groundwaters, and rivers exhibit very similar concentrations of all major elements, pH, and DOC. Only the most upper soil horizons formed by moss litter (0–5 cm, samples 18a and 18b) exhibit ~3 U lower pH values; the waters from swamp zones are slightly more acidic than neighboring rivers and groundwaters (samples 3, 28, 57). No distinct differences in chemical composition of interstitial solutions extracted from different soil horizons and between soil pore waters (samples 28, 48, 55, 71a, 71b, 85a, 85b) and underlying groundwaters (samples 30, 32, 75, 81, 84, 89, 92) have been observed.

To quantify the extent to which these solutions were supersaturated or undersaturated with respect to a given solid phase, we have calculated their saturation index Ω (for a given solid, Ω is defined as the ratio of the ion activity product in solution to the solubility product constant) using the MINTEQA2/PRODEFA2 chemical speciation code (Allison et al., 1991) and MINTEQA2 thermodynamic database (Nordstrom, 1990; Allison and Perdue, 1994). For this calculation, average values of major element concentrations in rivers, groundwaters, soil pore waters, and swamp zones were used. Because Al and Fe are mostly present in colloidal form, we used their concentrations measured in 1 kD (~1 nm) ultrafiltrates, even though 50 to 80% of organic carbon that can complex the metal ions remains in <1 kD pool (Pokrovsky et al., 2005c). All surficial fluids sampled in this work are close to equilibrium with respect to chalcedony SiO_2 (log Ω ~0.1); gibbsite $Al(OH)_3$ (0.2< log Ω < 0.4); imogolite $Al_2SiO_3(OH)_4$ (0.1 < log Ω < 0.3); allophanes $Al_2O_3(SiO_2)_{1-1.6} \cdot 2.5H_2O$ (-0.2 < log Ω < 0.2); halloysite $Al_4[Si_4O_{10}](OH)_8 \cdot nH_2O$ (log Ω ~0); and amorphous goethite (log Ω ~1). In agreement with all solutions being near equilibrium with amorphous Al-Si-bearing phases and amorphous iron hydroxides, aqueous silica as well as "dissolved" aluminum and iron concentrations in rivers are independent of river discharge and flooding events, both on long-term (Figs. A1-1B, A1-2B, A1-3B, A1-4B, A1-5B of the Appendix 1) and

Table 3. Chemical composition of soil porewaters (sp) and groundwaters.

Sample	Description	T, °C	pH	DOC μM	HCO_3 μM	Cl μM	SO_4 μM	Si μM	Na μM	K μM	Mg μM	Ca μM	Al μM	Fe μM
N 18a	sp A0, moss, plateau 200 m above the river	20	4.39	3217	233	1022	12.65	112	760.9	223.1	53.5	91.8	1.4	1.2
N 18b	sp A0, moss, plateau 200 m above the river	18	3.93	3292	10	247	1.84	39	210.4	11.5	27.2	44.7	2.8	0.8
N 8	sp/ground ice 50–60cm, *Larix g.,* moss	7	6.05	3467	51	16	6.12	289	113.0	7.7	78.2	134.0	7.4	4.9
N 17a	sp/ground ice 80 cm. under *Equisetum a.,* 1st terrace	18	7.70	3200	852	165	100.0	436	309	10.3	156	392	2.2	2.9
N 17b	sp 5–15 cm under *Equisetum a.,* 1st terrace	19	7.47	1325	531	69	46.9	375	135	20.5	99	186	1.1	1.6
N 23b	sp 40–80 cm. *Larix g.,* valley slope	4.5	7.67	1275	790	62	28.6	339	200	2.6	152	181	0.9	0.9
N 24	sp 40–50 cm permafrost; 1st terrace	0	7.68	1583	621	319	76.5	414	257	10.3	333	370	1.1	1.7
N 26	sp 40 cm, *Larix g.,* moss, terrace/ swamp	5	6.95	5275	1339	7	18.4	368	187	2.6	313	325	1.5	1.9
N 85a	sp 15–30 cm from swamp on terrace. *Larix g.* + *Betula p.*	10	7.06	1050	451	11	4.1	864	74	0.0	119	97	4.1	2.3
N 85b	sp/ground ice 80–150 cm over permafrost	5	7.64	642	815	7	3.1	482	117	2.6	148	228	1.0	1.4
N 71a	sp 30–50 cm under *Betula p.*	5	6.37	1342	274	9	4.1	207	43	7.7	66	77	6.3	2.1
N 71b	sp 10–20 cm under *Larix g.* and moss	10	7.79	1883	1080	15	6.1	479	178	2.6	259	295	3.7	4.9
N 48a	sp 0–10 cm on plateau, *Larix g.,* moss, lichens	3	6.75	1033	133	3	3.1	289	43	2.6	33	52	32.7	2.2
N 48b	sp/groundwater 10–20 cm on the valley slope	5.5	7.26	1275	284	3	2.0	254	48	2.6	70	82	3.7	2.0
N 55	sp 20 cm from 1st terrace of basaltic canyon	8.5	7.48	833	321	42	10.2	429	48	28.2	82	84	11.7	5.1
N 3	small creek from moss swamp. sphagnum	4.5	7.07	1817	574	6	4.1	275	109	2.6	123	201	8.7	9.0
N 4	sp 20–30 cm from moss swamp, *Larix g.*	15	6.69	2275	210	3	5.1	314	87	5.1	74	119	16.5	7.6
N 15	sp 0–2 A horizon on wet swamp, *Larix g.*	5	7.15	1967	207	2	0.0	207	48	2.6	86	92	10.5	3.9
N 28	sp 0–5 cm A0, moss, sphagnum swamp	30	6.88	1300	420	21	1.0	282	78	10.3	107	124	3.3	3.7
N 57	Surface water from moss swamp	12	6.22	2308	420	10	1.4	218	43	2.6	144	112	30.3	20.1
N 30	groundwater under basalt outcrop	7.5	7.33	1267	343	6	3.1	271	87	2.6	70	107	6.9	2.5
N 32	groundwater under permafrost. Moss, lichen, *Larix g.*	9	7.70	1083	456	3	1.0	200	74	2.6	86	179	3.0	1.8
N 75	groundwater from swamp on permafrost	6.5	7.33	1300	520	6	2.0	271	78	2.6	91	208	2.3	1.9
N 81	groundwater from valley slope, boulders	8	7.25	933	754	6	19.4	221	122	7.7	156	213	1.6	1.0
N 84	groundwater between massive basalt and porous tuffs	11	8.02	783	1130	9	2.0	336	174	5.1	177	253	1.1	0.9
N 89	ground/soil water over permafrost from No. 85	6	7.48	1750	772	12	3.1	264	161	5.1	177	221	1.2	1.6
N 92	ground/soil water similar to No. 89	7	7.68	1458	666	3	6.1	325	170	2.6	107	218	4.4	3.9
N 101	Permafrost (vein ice), 1.5 m depth	0	7.50	950	1270	15	2.0	175	274	10.3	226	313	1.4	2.3

Table 4. Mean multi-annual fluxes of elements, cationic weathering rate (TDS_c for sum of Ca, Mg, and Na + K fluxes), chemical weathering rate (TDS_w for sum of TDS_c, SiO_2, and SO_4), inorganic CO_2 consumption rate (R_{CO_2}), and suspended matter fluxes (R_{SM}) for rivers of studied region. All fluxes are corrected for atmospheric precipitation (section 2.2). The values correspond to basin (territory) weathering rates; the overall basalt weathering rates are 15 ± 5% lower. Uncertainty on the fluxes and runoffs is ±15–20% of the value except for R_{SM} which can vary by a factor of 1.5–2 depending on precipitation of the year. N.D. = non determined.

River	Runoff, mm/yr	Flux Si, t/km²/y	Flux Ca, t/km²/y	Flux Mg, t/km²/y	Flux Na + K, t/km²/y	TDS_c, t/km²/y	TDS_w, t/km²/y	Flux DOC, t/km²/y	R_{CO_2}, mol/km²/y	R_{SM}, t/km²/y
N. Tunguska, Tura (A)	205	0.94	2.38	0.38	1.73	4.5	6.9	1.6	$0.83 \cdot 10^5$	6.5 ± 2.0
N. Tunguska, B. Porog (D)	264	1.06	3.77	0.60	3.31	7.7	10.5	2.1	$1.23 \cdot 10^5$	N.D.
Tembenchi (B, No 90)	434	2.3	3.18	0.35	1.97	5.5	11.2	4.7	$1.0 \cdot 10^5$	N.D.
Eratchimo (E)	516	1.6	7.39	1.35	10.2	19.0	27.2	N.D.	$3.28 \cdot 10^5$	9.0 ± 1.5
Taimura (C, No 5)	205	1.2	3.01	0.54	2.22	5.8	10.3	3.3	$1.46 \cdot 10^5$	3.1 ± 0.5

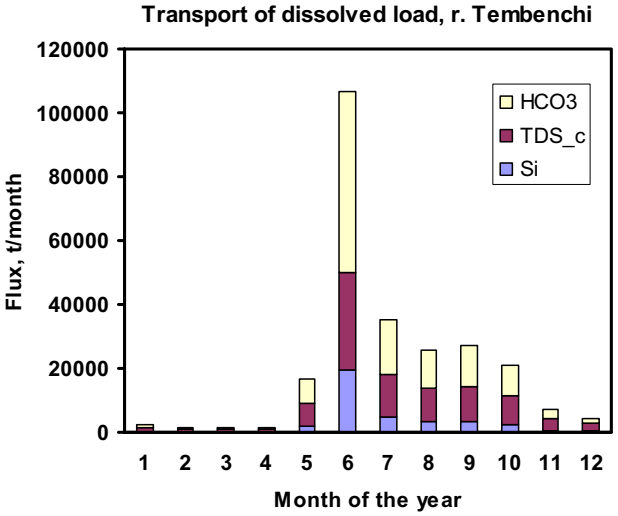

Fig. 6. Mean monthly fluxes (multiannual average for 1963–1980) of HCO_3, TDS_c and Si for Tembenchi River (B, N 90).

short-term (samples 83, 86 and 87) scales. This contrasts with alkaline and alkaline-earths, whose concentrations are dependent on river discharge. It should be noted that surficial solutions are strongly supersaturated ($\Omega > 100$) with well-crystallized clay minerals (kaolinite, nontronite, and montmorillonite), which is in agreement with field observations showing that clay-mineral precipitation is not important and thus has a weak impact on the budget of major cations. Overall these results are consistent with those of Gislason et al. (1996) and Stefansson and Gislason (2001) for rivers and groundwaters draining basaltic rocks in Iceland.

4. DISCUSSION

4.1. Sources of Elements in Rivers: Rocks, Soil, Litter, Underground Reservoirs, and Permafrost Ice

A ternary diagram of rocks, soil, rivers, groundwaters, soil pore waters, and plant litter in Ca-Mg-(Na + K) molar coordinates is presented in Figure 8A, whereas the binary diagram Ca/(Na + K) versus Mg(Na + K) is shown in Figure 8B. It can be seen in these figures that summer 2001 compositions of all

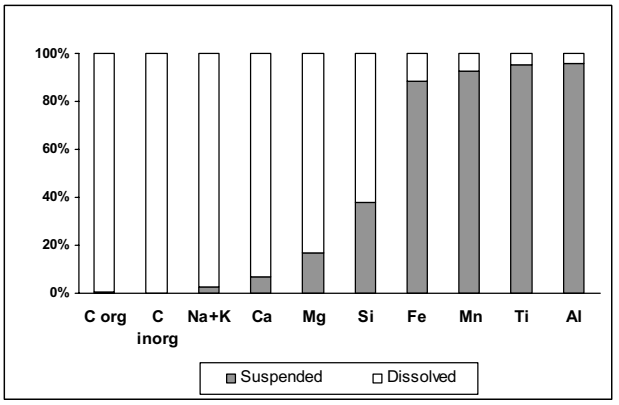

Fig. 7. Suspended versus dissolved transport in Taimura River (C, N 5).

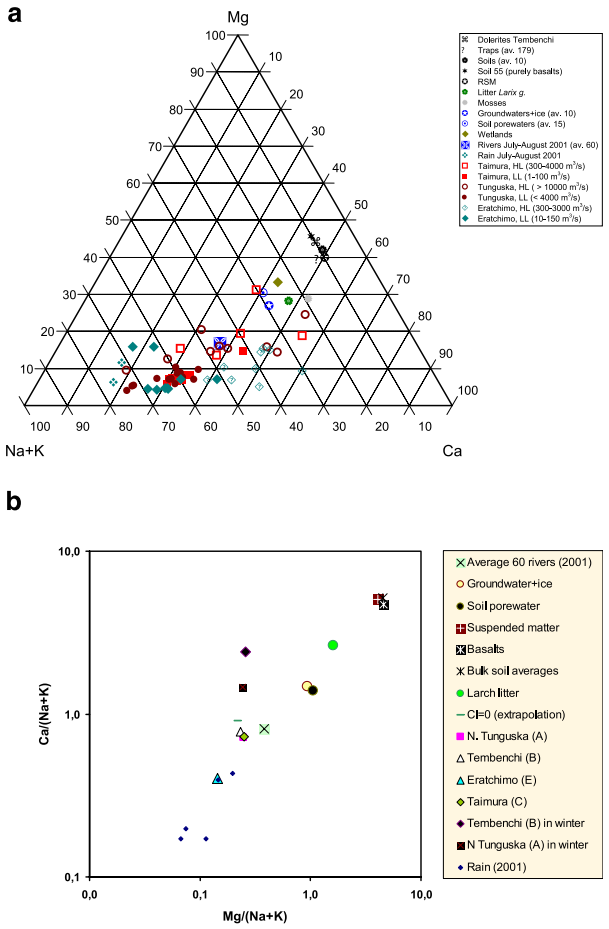

Fig. 8. (a) Ternary molar diagram of surface waters, rocks, soil and plant litter composition for studied region. HL = high level, LL = low level. (b) Binary molar diagram of surface waters, rocks, soil and plant litter composition for studied region. The data for Tunguska, Tembenchi, Eratchimo and Taimura rivers are mean multiannual values measured by the Russian Hydrological Survery. Cl = 0 corresponds to extrapolation of [Ca]/[Na + K], [Mg]/[Na + K] vs. [Cl] dependencies to [Cl] = 0 when the contribution of saline underground reservoir to the mean multiannual value is absent.

studied rivers (average of 60) lay between rocks and soils, plant litter, and precipitation, and they are similar to mean multiannual values for four large rivers studied by the Hydrological Survey. All solutions are enriched in alkali compared to basalts and soils. Moreover, in wintertime, which corresponds to the lowest discharge, and, thus, the lowest water/rock ratio, rivers are closer to the Na + K apex (Fig. 8A) and enriched in Ca versus Mg (Fig. 8B). This confirms the order of the mobility of the elements during chemical weathering (Na, K > Ca > Mg) deduced earlier in this study from the comparison of dissolved and suspended matter fluxes, but also indicates the presence of highly concentrated groundwater/salt deposits, mostly pronounced in wintertime for the river Tembenchi (see below). Soil pore waters, swamp waters, and river waters with the highest discharge (corresponding to spring melt and summer/autumn rains, and thus, the highest w/r ratio) are clustered towards the area representative of the upper soil horizons, with plant litter and moss. This probably reflects the important contribution of degrading litter. Note that during this period of the year, rivers become very rich in dissolved organic carbon (Fig. A2 of Appendix 2). This is likely to result from DOC washing out from plant debris and litter degradation products in the upper soil horizons, similar to that recently shown for European boreal zones (Land and Ohlander, 2000; Ingri et al., 2005). In summertime, a source of dissolved elements for rivers can be the release of fluids from soil pores and the groundwater reservoirs, which are progressively replaced by fresh rain of low mineralization, a process observed in tropical, temperate, and boreal watersheds (Viers et al., 2000; Olivie-Lauquet et al., 2001; Pokrovsky and Schott, 2002; Rember and Trefry, 2004; Pokrovsky et al., 2005a). However, we did not observe significant evolution of soil and groundwater composition between the low water period (July 25–August 10; samples 1–40 in Table 1) and the summer rain event lasting 2 to 3 weeks (samples 41–100).

High cation concentrations measured in rivers during winter can be explained by the dissolution of rock and soil minerals under low w/r ratio. This becomes possible due to the presence of unfrozen capillary water film (Anderson and Tice, 1973), whose formation is favored in organic-rich soils as the soil antifreeze capacity increases with increasing humus content (Sparrman et al., 2004). In wintertime, the contribution of deep groundwaters and salt (evaporate) deposits cannot be ruled out. Salt deposits are not reported in the studied region except in the very low strata of low Cambrian or Devonian evaporates that might be located at the depth of ~1000 to 1500 m. This contribution is especially pronounced in the river Tembenchi (see Appendix A1-3), whose total salt concentration in winter achieves 2.2 g/L due mostly to NaCl contribution. However, even for this river, the relative input of underground reservoir or salts to annual fluxes does not exceed 10.5%, as calculated from seasonal measurements of discharge and chemical composition from November to April (Fig. 6). For Eratchimo (E), Taimura (C) and Nizhniya Tunguska (D), Cl^- and HCO_3^- exhibit similar dependence of concentration on discharge. This would not be the case if Na(Ca, Mg) chloride and bicarbonate originated from different sources. Freezing of porous saturated rocks and surface waters followed by downward migration of concentrated fluids can be responsible for the origin of this underground reservoir. Note that in many Siberian permafrost regions, the presence of salty, highly mineralized (NaCl, $Ca(HCO_3)_2$) deep groundwaters formed during freezing of sands and sandstones is ubiquitous (Anisimova, 1981 and references therein). In the Putorana region, the tuffs underlying basalts may serve as such a porous reservoir capable of accommodating salt solutions that manifest themselves during the winter. Unfortunately, direct information on salt solutions or mineral deposits based on deep drilling in this region is not available.

To further test the evaporite input to river-water composition on the annual scale, we traced Ca, Mg, and HCO_3 mean multiannual concentrations normalized to [Na + K] as a function of mean [Cl^-] for four rivers from the Hydrological Survey database, after corrections for the atmospheric input. No dependence of [Mg] and [HCO_3] on [Cl] was found. A semilinear dependence observed for Ca allowed extrapolation of these relationships to [Cl] = 0, and thus, determination of [Mg]/[Na + K], [Ca]/[Na + K] in rivers of the territory corrected for the presence of salt deposits. This value was

found to be similar to our summer 2001 measurements for 60 rivers, and to the average annual composition of major rivers (Fig. 8B).

In summertime, clear evaporitic signatures can be detected only for the river Nidym (N 20), in which Cl concentration achieves 76 mg/L. For most small and medium rivers of the region and all soil pore waters and shallow groundwaters sampled in 2001, chloride concentration does not exceed 2 mg/L, comparable to that measured in the rain. Large rivers Kochechumo (N 1), Yambukan (N 2), Taimura (N 5), Nizhniya Tunguska (N6), Vivi (N 7), and Ganalchik (N 19) sampled during relatively low-water period in summer 2001 (July 25–July 30) contain elevated concentrations of sodium and calcium chloride (10–20 mg Cl/L). The river Kochechumo sampled one month later after an extensive rain period (N 96) exhibits much lower Cl concentration. Therefore, similar to the study of Moulton et al. (2000) for Iceland, it is reasonable to assume that no Cl^- in rivers is contributed by basaltic rock weathering, given the low Cl concentrations in Siberian traps (90 ppm vs. 200 ppm in Iceland; Zolotukhin and Al'Mukhamedov, 1988). The most probable explanation for high Cl concentration in large rivers during dry summer period is its origin from the deep groundwaters that are exposed on the bottom of the deep valleys of these rivers.

Results of this study show that, besides bedrocks and soil minerals, the main sources of dissolved elements can be degraded plant litter and permafrost thawing. The contribution of plant litter can be assessed from the analysis of litter elementary composition (Table 1). The annual net primary productivity (NPP) for the region is 90 g C/m^2 at Tura in 1998 (Kajimoto et al., 1999). The crucial parameter for estimating litter impact is the ratio between the export flux (J) of the elements from degrading litter and the primary production (NPP). The J/NPP ratio is extremely low for biogenic elements such as P, K, N, and C (0.01–0.02), but reaches 0.88 for mineral components in the taiga region (Bazilevitch, 1976; Savenko, 2004). Thus, for TDS_c = Na + K + Ca + Mg we will consider the range of J/NPP between 0.1, as for overall detritus production (Vogt et al., 1982; Schlesinger, 1997) and 0.88. Assuming steady-state conditions of forest biomass and soil thickness, and converting to element content in the dry biomass using data from Table 1, this yields for Si, Ca, Mg, Na, Fe, and Al minimal values of annual fluxes issued from litter degradation equal to 0.34, 0.17, 0.06, 0.016, 0.09, and 0.1 t/km^2/yr, respectively. The maximal values may be ~9 times higher.

Interestingly, the element fluxes issued from natural degradation of litter are comparable with those induced by forest fires. Shvidenko and Nilsson (2002) estimated that 25 tons C/km^2/yr are lost by direct and indirect effects of fire in Russia. Converting this value into 50 t/km^2/yr dry plant biomass, and taking into account the typical element content in larch and coniferous trees that are mostly subjected to fire events (e.g., ~1% of Ca, Table 1; Kovda, 1956), gives ~0.5 t Ca/km^2/yr related to forest fires. Considering (i) the catastrophic character of fire events, (ii) the rapid dissolution in surficial fluids and washout of the ash products, and (iii) accelerated permafrost melting due to intense ground heating, the concentrations of elements issued in the rivers from these phenomena can be, locally, much higher than those originated from chemical erosion in soils, and thus, they deserve further studies.

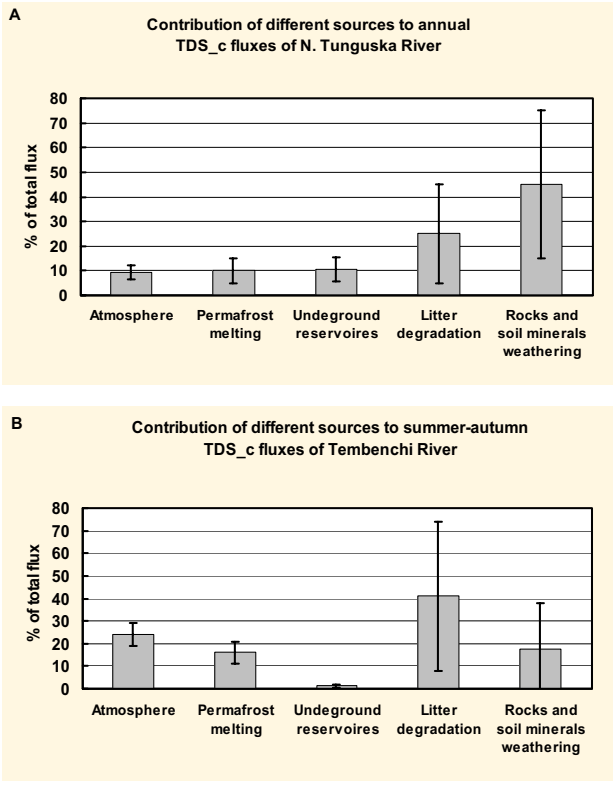

Fig. 9. Contribution of different sources to annual (A) and summer-autumn (July to October, B) fluxes of total dissolved cations (Ca + Mg + Na + K) of N. Tunguska and Tembenchi rivers.

A third potential source of elements in rivers during warm high-water season is the permafrost thawing. Concentrations of all major elements and DOC in vein permafrost ice (sample 101, Table 4) and in ground ice (samples 8, 17a, 85b, Table 4) are comparable or higher than those in soil pore waters, groundwater, and rivers. To approximate the potential impact of permafrost ice thawing on river chemistry, we have hypothesized that 40 ± 20 cm of soil active layer having ~5% of ground ice, as follows from our field data on water proportion in frozen samples of deep soil horizons (see section 2.3), can thaw during the summertime. This gives a values of TDS_c flux issued from permafrost melting of 0.5 ± 0.15 t/km^2/yr.

Based on these data, we estimated the relative proportion of various sources to river cationic composition, both on annual and summer-autumn timescale (July–October; Fig. 9). For this, we used multiannual data of atmospheric precipitates (75% occurs in August–September) and uncorrected fluxes (F_{tot}) calculated by Eqn. 2 (section 2.2). We also assumed that the underground input ($F_{underground}$) is constant over the year, but dominates the river cationic discharge only in the wintertime (November–April). The contribution of salts to summertime river composition can be approximated by comparison of Cl concentration in rivers in summer (i.e., 8.25 mg/L for Tembenchi) and in winter (400–1300 mg/L), which yields the contribution of groundwater equals to ~1.3 ± 0.7%. Therefore, the overall role of possible salt minerals in determining the relative mobility of elements (i.e., Fig. 7 and section 3.2.1) is negligible because such a mobility diagram is based on summer and

average multiyear annual data. Finally, we assumed that the permafrost thawing ($F_{permafrost}$) and the litter degradation (F_{litter}) occur during summer-autumn (July–October). Therefore, the overall flux is given as

$$F_{tot} = F_{atmosphere} + F_{underground} + F_{litter} + F_{permafrost} + F_{RW} \quad (3)$$

where F_{RW} is direct basalt and soil mineral chemical weathering via rock-water interaction with soil pore water fluids. It can be seen from Figure 9 that both during the active period and on the annual scale, the largest uncertainty stems from litter degradation processes, precisely, the *J*/NPP value. The exact contribution of direct mobilization of elements from the rocks is not possible to assess, it ranges between 20 and 70% of total river TDS_c flux.

In a thorough study of oxygen isotope composition of Siberian permafrost ice, Nikolayev and Mikhalev (1995) show that precipitation and snowmelt is the dominant source of moisture for both surface ground ice and deep ice veins. One thus can propose the following general scheme of solutes migration over the annual cycle. After intensive washout of plant debris, litter, and minerals and organic matter from the uppermost soil horizon during the snowmelt (end of May–June), the source of surface waters becomes atmospheric precipitation (rain) and ground ice thawing (July–August). During this warm period, the downward penetrating rainwaters interact with the litter and upper soil horizons and further migrate along the permafrost table to the rivers. However, because the depth of the active layer increases during this period, part of the migrating fluids is being trapped in soil pores and pockets of the progressively defreezing layer. At the end of the active period (August–September), when most of precipitation occurs, this fluid-saturated layer achieves the highest depth. In these environments, solutions stay enough time in contact with degrading litter and soil minerals to be enriched in all major and trace elements, including organic carbon. At the beginning of the cold period, the freezing of soil fluids in a confined space cannot lead to freezing front migration, and no distillation occurs. As a result, the chemical composition of ground ice or ice vein is similar to that of soil pore waters or groundwater, without significant chemical evolution. During the next warm period, after the snowmelt, thawing of this "last-year" ground ice again may serve as an important source of both water and solutes to the rivers.

4.2. CO_2 Consumption Rates and the Chemical Erosion Intensity in the Siberian Platform

The inorganic CO_2 consumption rate for Siberian traps can be calculated from HCO_3^- concentration, assuming that all bicarbonate in the river, after correction for the atmospheric input, is originated from silicate weathering (direct or indirect via plants). For the largest river of the region (Nizhniya Tunguska at Bolshoi Porog), the CO_2 consumption rate is $0.08 \cdot 10^{12}$ mol/yr or 1.4 t/km^2/yr, which represents only 2.6% of the annual consumption flux during basalt weathering at the Earth's surface, in agreement with previous estimations of Dessert et al. (2003). DOC fluxes of studied rivers (2–4 t/km^2/yr) are comparable with mean multiannual organic carbon fluxes for large Russian Arctic rivers (Gordeev et al., 1996). The fate of this DOC in the Arctic estuarine zones is poorly known; however, it is possible that a significant part of plant-originated organic carbon is buried in the river mouth zone (Guo et al., 2004; Romankevich and Vetrov, 2004).

Several factors can be considered to control the chemical erosion of Siberian basalts. The presence of highly soluble minerals in trace amounts in the rocks (i.e., carbonates: Anderson et al., 1997; White et al., 1999; White et al., 2005 Ca-plagioclases: Oliva et al., 2004) is known to strongly affect the intensity of chemical weathering and the fluxes of major ions. The presence of calcite traces such as in the Deccan basalts (Das et al., 2005) cannot be totally ruled out, although calcite was never detected from microscopic observations of thin sections of fresh rocks. Weak abundance of calcite is also supported by XRD analysis of soil and sediments and fine fraction of rocks; traces of, presumably, pedogenic calcite were detected (soils 28a and 47) in only two cases. On the binary diagram (Fig. 8B), however, there is no shift of summer 2001 and mean multiannual river-water compositions towards carbonate pole, which suggests negligible effect of the presence of calcite traces on overall basin weathering rates.

In the permafrost region, an important weathering agent can be cryoturbation, driven by repeated freezing and thawing that creates highly contorted soil horizons and constitutes a pedogenic process typical of the cold regions (Retzer, 1965; Tedrow, 1974; Ugolini, 1986), where the frost mixing within the soil profile can supply fresh minerals to the upper reactive horizons (Targulian, 1971; Hall et al., 2002). In such environments, freezing front migration downwards leads to irreversible changes in the soil structure and to transformation and neoformation of clay minerals within the active layer (Zvereva and Ignatenko, 1983; Konischev and Rogov, 1993; Polubesova et al., 1996; Vogt and Larqué, 1998; Hoch et al., 1999; Alekseev et al., 2003). For Putorana traps, the physical impact of permafrost on rocks leads to well mixing of the soil profile and to separation of primary smectite that accumulates in soils and constitutes an essential part of river suspended matter.

Dissolved organic carbon has been widely reported as a potentially important catalyst of silicate rock weathering (Drever, 1994; Viers et al., 1997; Oliva et al., 1999; Gaillardet et al., 2003; Millot et al., 2002; Millot et al., 2003; Zakharova et al., 2005). A direct effect of DOC on the weatherability of Siberian basalts could not be detected. First, there is no correlation between the major element and DOC concentrations for 60 large and small rivers of the region, for example, the most northern rivers, Yagdali (N 29) and Kochechumo (N 27), exhibit very low [DOC] but [TDS_c] and [HCO_3^-], which are similar to those of organic-rich southern rivers (Vivi N 7, Yambukan N 2). Second, over the annual cycle, the major cations and DOC concentrations exhibit opposite dependences on river discharge; the [TDS_c] decreases but [DOC] strongly increases with discharge increase (Appendix 2 for DOC and Figs. A1-1 to A1-5 of Appendix 1 for cations). Because there is no correlation between DOC and dissolved cation concentrations, both in the low and high water period, it is unlikely that DOC directly affects aqueous and surface speciation of major cations and controls their release from rocks and soil minerals. This observation is consistent with recent results from our laboratory, which show a rather weak effect of dissolved organic matter such as soil carboxylic and aromatic com-

pounds, chemical analogs of cell envelopes and microbial exudates, and natural humic and fulvic acids at their concentrations as high as 0.001 to 0.01 M, on base cations and silica release rate from Ca, Mg-bearing oxides and silicates such as brucite, diopside, wollastonite, and smectite (Golubev et al., 2004; Pokrovsky et al., 2004; Pokrovsky et al., 2005b). In contrast, the strong effect of organic ligands on dissolution rates of alumosilicates (feldspars and glass) at 10^{-5} to 10^{-4} M concentrations (Drever and Stillings, 1997; Oelkers and Schott, 1998; Oelkers and Gislason, 2001) and on Fe and trace element mobilization from basalt (Neaman et al., 2005a; Neaman et al., 2005b) are well-established.

5. CONCLUSIONS

The present study allows quantitative characterization of the chemical erosion of basic rocks in permafrost-dominated boreal regions of Central Siberia. Overall basin weathering fluxes estimated from long-term and short-term analysis of the chemical composition of rivers are among the lowest in the world (TDS_c = 5–6 t/km^2/yr). The order of element mobility during weathering inferred both from solution and solid chemistry ($C_{inorg} \geq C_{org} > Na > Ca > K, Mg > Si > Fe \geq Mn \geq Ti \geq Al$) is similar to that established for other regions of the world. In general accord with soil-forming processes on sedimentary or acid metamorphic rocks in permafrost-dominated environments under cold continental climate (e.g., Naumov and Gradusov, 1974), the weathering of basic rocks in the studied region does not lead to chemical and mineralogical differentiation along the soil profile. The clay minerals of the soil and river suspended sediments are represented by illite-smectite (chlorite) minerals originated from the parent rocks that replace original olivines and basaltic glass. This study, in accord with previous literature data, did not reveal abundant formation of contemporary authigenic clay minerals, but rather, the presence of amorphous allophanes and Fe-Al-organic compounds. Over the full period of the year, semiconstant Si, Fe, and Al concentration in rivers reflects their saturation with secondary amorphous phases such as allophanes, iron, and aluminum hydroxides.

The chemical composition of rivers during the high-level period, when most of the annual element flux occurs, approaches that of plant litter and upper soil horizons, suggesting intensive surface leaching of cations from soil organic substances, such as the case for other boreal watersheds (e.g., Ingri et al., 2005). During the low-level period in winter, the contribution of parent rocks and soil minerals is responsible for the enrichment of rivers in most labile elements like alkalis, while the input of saline (Na-Cl-Ca-HCO_3) underground reservoirs can be recognized for large rivers. However, the contribution of this underground reservoir to the annual element fluxes does not exceed 10%. During the unfrozen period of the year, contribution from plant litter, soil clay minerals, and permafrost ground and ice veins becomes important. From the beginning of the active period, downward penetrating fluids interact with degrading litter and secondary minerals in upper soil horizons, leaching the major and trace elements. At the beginning of the cold period, full freezing of soil pore solutions without important chemical separation can occur. This ground (permafrost) ice, located within 0.5 to 1.5 m below the surface, can serve as a potential pool of solutes during the next warm period. In accord with this, no strong chemical differentiation between soil pore waters, groundwater, and permafrost ice has been detected, and the chemical composition of these "ground" fluids resembles that of river waters.

Acknowledgments—This work was supported by the French program PNSE (Program National "Sol et Erosion") jointly funded by INSU/CNRS agencies. We thank Associate Editor Dr. Krishnaswami and three anonymous reviewers for their helpful comments that greatly improved the presentation and interpretation of our results. The invaluable help of B.G. Pokrovsky, during fieldwork and for providing geological information, is acknowledged. We thank A. P. Abaimov and S. V. Prokushkin for accommodating us on the scientific station of Tura and for useful discussions. E. A. Zakharova is thanked for great help with preparation of the maps of the studied region.

Associate editor: S. Krishnaswami

REFERENCES

Abaimov A. P., Bondarev A. I., Zyryanova O. A., and Shitova S. A. (1997) *Polar Forests of Krasnoyarsk Region.* Nauka (in Russian).

Alekseev A., Alekseeva T., Ostroumov V., Siegert C., and Gradusov B. (2003) Mineral transformations in permafrost-affected soils, North Kolyma Lowland, Russia. *Soil Sci. Soc. Amer. J.* **67,** 596–605.

Allison J. D. and Perdue E. M. (1994) Modeling metal-humic interaction with Minteqa2. In *Humic Substances in the Global Environment and Implications on Human Health* (ed. N. Senesi and T. M. Miano), pp. 927–942, Elsevier Science B.V.

Allison J. D., Brown D. S., and Novo-Gradac K. J. (1991) *MINTEQA2/PRODEFA2, A Geochemical Assessment Model for Environmental Systems: Version 3.0 User's Manual.* U.S. Environmental Protection Agency.

Anderson D. M. and Tice A. R. (1973) The unfrozen interfacial phase in frozen soil water systems. In *Physical Aspects of Soil Water and Salt in Ecosystems* (ed. A. Hadas), pp. 107–124, Springer Verlag.

Anderson S. P., Drever J. I., and Humphrey N. F. (1997) Chemical weathering in glacial environments. *Geology* **25,** 399–402.

Anisimova N. P. (1981) *Cryohydrochemical Features of Permafrost Zone. (Kriogidrokhimicheskie osobennosti merzloi zony).* Nauka (in Russian).

Bazilevitch N. I. (1976) Biogenic and abiogenic processes in forest, step and desert ecosystems. *International Geography* **76,** 58–62.

Benedetti M. F., Menard O., Noack Y., Carvalho A., and Nahon D. (1994) Water-rock interactions in tropical catchments: field rates of weathering and biomass impact. *Chem. Geol.* **118,** 203–220.

Berner R. A. (1992) Weathering, plants and the long-term carbon cycle. *Geochim. Cosmochim. Acta* **56,** 3225–3231.

Botch M. S., Kobak K. I., Vinson T. S., and Kolchugina T. P. (1995) Carbon pools and accumulation in peatlands of the former Soviet Union. *Global Biogeochem. Cycles* **9,** 37–46.

Brady P. V., Dorn R. I., Brazel A. J., Clark J., Moore R. B., Glidewell T. (1999) Direct measurement of the combined effects of lichen, rainfall and temperature on silicate weathering. *Geochim. Cosmochim. Acta* **63,** 3293–3300.

Chesworth W., Dejou J., and Larroque P. (1981) The weathering of basalt and relative mobilities of the major elements at Belbex, France. *Geochim. Cosmochim. Acta* **45,** 1235–1243.

Courtillot V. E. and Renne P. R. (2003) On the ages of flood basalt events. *C.R. Geoscience* **335,** 113–140.

Dainyak L. G., Dritz V. A., Kudryavtzev D. I., Simanovitch I. M., and Slonimskaya M. V. (1982) New mineral form of trioctahedric smectite from effusive basalts of Tungusskaya sineclise. *Lithology Mineral Res.* **6,** 123–129.

Das A., Krishnaswami S., Sarin M. M., and Pande K. (2005) Chemical weathering in the Krishna basin and Western ghats of the Deccan Traps, India: Rates of basalt weathering and their controls. *Geochim. Cosmochim. Acta* **69,** 2067–2084.

Dessert C., Dupré B., François L. M., Schott J., Gaillardet J., Chakrapani G. J., and Bajpai S. (2001) Erosion of Deccan Traps

determined by river geochemistry: impact on the global climate and the $^{87}Sr/^{86}Sr$ ratio of seawater. *Earth Planet. Sci. Lett.* **188,** 459–474.

Dessert C., Dupré B., Gaillardet J., François L. M., and Allègre C. J. (2003) Basalt weathering laws and the impact of basalt weathering on the global carbon cycle. *Chem. Geol.* **202,** 257–273.

Drever J. I. (1994) The effect of land plants on weathering rates of silicate minerals. *Geochim. Cosmochim. Acta* **58,** 2325–2332.

Drever J. I. and Stillings L. L. (1997) The role of organic acids in mineral weathering. *Colloids Surfaces A* **120,** 167–181.

Drits V. A. and Sakharov B. A. (1976) *X-Ray Diffraction Analysis of Mixed-Layer Minerals.* (Rentgeno-Structurnyi Analyis Smeshanno-Sloiknukh Mineralov). Nauka. (in Russian).

Drits V. A., Sakharov B. A., Dainyak L. G., Salyn A. L., and Lindgren H. (2002) Structural and chemical heterogeneity of illite-smectite from Upper Jurassic mudstones of East Greenland related to volcanic and weathered parent rocks. *Amer. Mineral.* **87,** 1590–1607.

Dupré B., Dessert C., Oliva P., Goddéris Y., Viers J., Francois L., Millot R., and Gaillardet J. (2003) Rivers, chemical weathering and Earth's climate. *C.R. Geoscience* **335,** 1141–1160.

Ershov Yu. I. (1994) Mesomorphic soil formation in cryogenic-taiga semihumid region of Central Siberia. *Pochvovedenie (Sov. Soil Sci.) N* **10,** 10–18.

Ershov Yu. I. (1995) Features of forest soil formation in the north of Central Siberia. *Pochvovedenie (Sov. Soil Sci.) N* **7,** 805–810.

FAO/UNESCO (1978) *Soil Map of the World 1 : 5000 000.* Vol. VIII, North and Central Asia. Sheets VIII-1, VIII-2 and VIII-3, Edition 1/1977. UNESCO, Paris.

Gaillardet J., Millot R., and Dupré B. (2003) Chemical denudation rates of the western Canadian orogenic belt: the Stikine terrane. *Chem. Geol.* **201,** 257–279.

Gislason S. R., Arnorsson S., and Armannsson H. (1996) Chemical weathering of basalt as deduced from the composition of precipitation, rivers and rocks in Southwest Iceland: effect of runoff, age of rocks and vegetative/glacial cover. *Amer. J. Sci.* **296,** 837–907.

Golubev S. V., Pokrovsky O. S., and Schott J. (2004) Laboratory weathering of Ca- and Mg-bearing silicates: Weak effect of CO_2 and organic ligands. Abstracts of the 13th annual V. M. Goldschmidt Conference. *Geochim. Cosmochim. Acta* **68,** A418 (suppl.).

Gordeev V. V. and Sidorov I. S. (1993) Concentration of major elements and their outflow into the Laptev Sea by the Lena River. *Marine Chemistry* **43,** 33–45.

Gordeev V. V., Martin J. M., Sidorov I. S., and Sidorova M. V. (1996) A reassessment of the Eurasian river input of water, sediment, major elements and nutrients to the Arctic ocean. *Amer. J. Sci.* **296,** 664–691.

Gradusov B. P. and Ivanov V. V. (1983) Mineralogical composition of clay minerals in soils of Putorana plateau. *Vestnik Mosk. Univer. Ser. 17 Pochvovedenie (Proceed. Moscow State Univ. Ser 17, Soil Science)* **1,** 44–51.

Guo L., Semiletov I., Gustafsson O., Ingri J., Andersson P., Dudarev O., and White D. (2004) Characterization of Siberian Arctic coastal sediments: Implications for terrestrial organic carbon export. *Global Biogeochem. Cycles* **18,** 1–11.

Hall K., Thorn C. E., Matsuoka N., and Prick A. (2002) Weathering in cold regions: some thoughts and perspectives. *Progr. Phys. Geogr.* **26,** 577–603.

Hinsinger P., Barros O. N., Benedetti M. F., Noack Y., and Callot G. (2001) Plant-induced weathering of a basaltic rocks: Experimental evidence. *Geochim. Cosmochim. Acta* **65,** 137–152.

Hoch A. R., Reddy M. M., and Drever J. L. (1999) The importance of mechanical disaggregation in chemical weathering in a cold, alpine environment, San Juan Mountains, Colorado. *Geol. Soc. Amer. Bull.* **111,** 304–314.

Hydrological Yearbooks of Russian Hydrological Survey, 1954-1975. Yenissey Basin. Vol. 7, parts 2–4. State Gidromet, Krasnoyarsk, 1975.

Ingri J., Widerlund A., and Land M. (2005) Geochemistry of major elements in a pristine boreal river system; Hydrological compartments and flow paths. *Aquatic Geochem.* **11,** 57–88.

International Organization for Standardization. (1983) *Liquid Flow Measurement in Open Channels,* Handbook 16, International Standards Organization.

Kajimoto T., Matsuura Y., Sofronov M. A., Volokitina A. V., Mori S., Osawa A., and Abaimov A. P. (1999) Above- and belowground biomass and net primary productivity of a *Larix gmelinii* stand near Tura, central Siberia. *Tree Physiol.* **19,** 815–822.

Konischev V. N. and Rogov V. V. (1993) Investigations of cryogenic weathering in Europe and Northern Asia. *Permafrost Periglacial Processes* **4,** 49–64.

Kovda V. A. (1956) Mineral composition of plants and soil formation. *Soviet Soil Sci.(Pochvovedenie)* **1,** 6–38.

Kudryavtzev D. I. (1979) On the alteration of interstitial glass in effusive basalts of Tungusskaya sineclise. *Lithology Mineral Res.* **2,** 139–144.

Land M. and Ohlander B. (2000) Chemical weathering rates, erosion rates and mobility of major and trace elements in a boreal granitic till. *Aquatic Geochem.* **6,** 435–460.

Lindgren H., Drits V. A., Sakharov B. A., Jacobsen H. J., Salyn A. L., Dainyak L. G., and Krayer H. (2002) The structure and diagenetic transformation of illite-smectite and chlorite-smectite from North Sea Cretaceous-Tertiary chalk. *Clay Minerals* **37,** 429–450.

Lurie M. L. and Masaitis V. L. (1958) Trapp formation. In *Geological Composition of the USSR*, Vol. 2 (ed.. Y. I. Polovinkin), pp. 254–260, Gosgeoltekhizdat (in Russian).

Millot R., Gaillardet J., Dupré B., and Allègre C. J. (2002) The global control of silicate weathering rates and the coupling with physical erosion: new insights from rivers of the Canadian Shield. *Earth Planet Sci. Lett.* **196,** 83–98.

Millot R., Gaillardet J., Dupré B., and Allègre C. J. (2003) Northern latitude chemical weathering rates: Clues from the Mackenzie River Basin, Canada. *Geochim. Cosmochim. Acta* **67,** 1305–1329.

Moulton K. L., West J., and Berner R. A. (2000) Solute flux and mineral mass balance approaches to the quantification of plant effects on silicate weathering. *Am. J. Sci.* **300,** 539–570.

Naumov E. M. and Gradusov B. P. (1974) *Specific Features of Taiga Soil Formation in the Extreme North-East Of Eurasia.* Koloss (in Russian).

Neaman A., Chorover J., and Brantley S. L. (2005a) Element mobility patterns record organic ligands in soils on early Earth. *Geology* **33,** 117–120.

Neaman A., Chorover J., and Brantley S. L. (2005b) Implications of the evolution of organic acid moieties for basalt weathering over geological time. *Amer. J. Sci.* **305,** 147–185.

Négrel P., Allègre C. J., Dupré B., and Lewin E. (1993) Erosion sources determined by inversion of major and trace element ratios and Sr isotopic ratios in river water. The Congo basin case *Earth Planet. Sci. Lett.* **120,** 59–76.

Nesbitt H. W. and Wilson R. E. (1992) Recent chemical weathering of basalts. *Amer. J. Sci.* **292,** 740–777.

Nikolayev V. I. and Mikhalev D. V. (1995) An oxygen-isotope paleothermometer from ice in Siberian Permafrost. *Quaternary Res.* **43,** 14–21.

Nordstrom D. K., Plummer N. L., Langmuir D., Busenberg E., May H. M., Jones B. F. and Parkhurst D. L. (1990) Revised chemical equilibrium data for major water-minerals reactions and their limitations. In *Chemical Modeling of Aqueous Systems II* (ed. D. C. Melchior and R. L. Bassett), vol. 416, pp. 398–413. American Chemical Society Symposium Series.

Oelke C., Zhang T. J., Serreze M. C., and Armstrong R. L. (2003) Regional-scale modeling of soil freeze/thaw over the Arctic drainage basin. *J. Geophys. Res.–Atmospheres* **108,** 4314.

Oelkers E. H. and Gislason S. R. (2001) The mechanism, rates and consequences of basaltic glass dissolution: I. An experimental study of the dissolution rates of basaltic glass as a function of aqueous Al, Si and oxalic acid concentration at 25°C and pH = 3 and 11 *Geochim. Cosmochim. Acta* **65,** 3671–3681.

Oelkers E. H. and Schott J. (1998) Does organic acid adsorption affect alkali-feldspar dissolution rates? *Chem. Geol.* **151,** 235–245.

Oliva P., Viers J., Dupré B., Fortuné J.-P., Martin F., Braun J.-J., Nahon D., and Robain H. (1999) The effect of organic matter on chemical weathering: Study of a small tropical watershed: Nsimi-

Zoétélé site, Cameroon. *Geochim. Cosmochim. Acta* **63,** 4013–4035.

Oliva P., Dupré B., Martin F., and Viers J. (2004) The role of trace minerals in chemical weathering in a high mountainous granitic watershed (Estibère, France): Chemical and mineralogical evidence. *Geochim. Cosmochim. Acta* **68,** 2223–2243.

Oliver B. G., Thurman E. M., and Malcolm R. L. (1983) The contribution of humic substances to the acidity of colored natural waters. *Geochim. Cosmochim. Acta* **47,** 2031–2035.

Olivié-Lauquet G., Gruau G., Dia A., Riou C., Jaffrezic A., and Henin O. (2001) Release of trace elements in wetlands: role of seasonal variability. *Water Res.* **35,** 943–952.

Peterson B. J., Holmes R. M., McClelland J. W., Vorosmarty C. J., Lammers R. B., Shiklomanov A. I., Shiklomanov I. A., and Rahmstorf S. (2002) Increasing river discharge to the Arctic Ocean. *Science* **298,** 2171–2173.

Pokrovsky O. S. and Schott J. (2002) Iron colloids/organic matter associated transport of major and trace elements in small boreal rivers and their estuaries (NW Russia). *Chem. Geology* **190,** 141–179.

Pokrovsky O. S., Golubev S. V., and Schott J. (2004) Impact of dissolved organics on mineral dissolution kinetics: Towards a predictive model for Ca- and Mg-bearing oxides, carbonates and silicates. Abstracts of the 13th annual V. M. Goldschmidt Conference. *Geochim. Cosmochim. Acta* **68,** A141 (suppl.).

Pokrovsky O. S., Dupré B., and Schott J. (2005a) Fe-Al-organic colloids control of trace elements in peat soil solutions: results of ultrafiltration and dialysis. *Aquatic Geochem.*, in press.

Pokrovsky O. S., Schott J., and Castillo A. (2005b) Kinetics of brucite dissolution at 25°C in the presence of organic and inorganic ligands and divalent metals. *Geochim. Cosmochim. Acta* **69,** 905–918.

Pokrovsky O. S., Schott J., and Dupré B. (2005c) Basalt weathering and trace elements migration in the boreal Arctic zone. *J. Explorat. Geochem*, in press.

Polubesova T. A., Shirshova L. T., Lefevre M., and Romanenkov V. A. (1996) Effect of freezing and thawing on the surface chemical properties of soils and clays. *Eurasian Soil Sci.* **28,** 104–114.

Polynov B. B. (1944) Modern objects of weathering study (Sovremennye zadachi ucheniya o vyvetrivanii). *Izv. Acad. Nauk SSSR, Ser. Geol.* **2,** 3–14.

Rember R. and Trefry J. (2004) Increased concentrations of dissolved trace metals and organic carbon during snowmelt in rivers of the Alaskan Arctic. *Geochim. Cosmochim. Acta* **68,** 477–489.

Resources of surface waters of the USSR. (1973) In *The Main Hydrological Characteristics. Yenisseisky Region,* Vol. 17 (ed. I. A. Zilbershtein and I. S. Stolyarchuk), p. 282. Leningrad, Gidrometeoizdat.

Retzer J. L. (1965) Present soil-forming factors and processes in arctic and alpine regions. *Soil Sci.* **7,** 22–32.

Romankevich E. A. and Vetrov A. A. (2004) *Carbon Cycle in the Russian Arctic Seas.* Springer.

Samoilov A. G. (1989) Chemical weathering of traps formation in subarctic conditions. *Dokl. Acad. Sci. USSR* **308,** 716–721.

Savenko V. S. (2004) *What Is The Life? Geochemical Approach to the Problem.* Moscow State University, GEOS Publishing House.

Schlesinger W. H. (1997) *Biogeochemistry. An Analysis of Global Change.* Academic Press.

Semenov A. D., ed. (1977) *Guide on the Chemical Analysis of Continental Surface Waters.* Gidrometeoizdat. (in Russian).

Serreze M. C., Bromwich D. H., Clark M. P., Etringer A. J., Zhang T. J., Lammers R. (2002) Large-scale hydro-climatology of the terrestrial Arctic drainage system. *J. Geophys. Res. – Atmospheres* **108,** 1–28.

Shvidenko A. and Nilsson S. (2002) Dynamics of Russian forests and the carbon budget in 1961–1998: An assessment based on long-term forest inventory data. *Climatic Change* **55,** 5–37.

Sokolov I. A. (1991) Some theoretical conceptions and problems in the investigations of East Siberian and Far East soils. *Pochvovedenie (Sov. Soil Sci.)* **5,** 131–145.

Sokolov I. A. and Bystryakov G. M. (1980) Pale-colored soils of Eastern Siberia and Far East northern taiga. *Vestnik Mosk. Univer. Ser. 17 Pochvovedenie (Proceed. Moscow State Univ. Ser. 17, Soil Science)* **1,** 30–37.

Sokolov I. A. and Gradusov B. P. (1978) Autonomous mesomorphic soil formation and weathering on basic rocks under conditions of a cold humid climate. *Pochvovedenie (Sov. Soil. Sci.)* **2,** 5–17.

Soyer V. G. and Semenov A. D. (1971) Photochemical method of organic carbon determination. *Gidrokhim. Materialy* **56,** 111–120. (in Russian).

Sparrman T., Oquist M., Klemedtsson L., Schleucher J., and Nilsson M. (2004) Quantifying unfrozen water in frozen soil by high-field ^{2}H NMR. *Environ. Sci. Technol.* **38,** 5420–5425.

Stefansson A. and Gislason S. R. (2001) Chemical weathering of basalts, Southwest Iceland: effect of rock crystallinity and secondary minerals on chemical fluxes to the oceans. *Amer. J. Sci.* **301,** 513–556.

Targulian V. O. (1971) *Soil Formation and Weathering in Cold Humid Regions (On Massive-Crystalline and Sandy Polymictic Rocks).* Nauka.

Tedrow J. C. F. (1974) *Soils of the Polar Landscapes.* Rutgers University Press.

Ugolini F. C. (1986) Processes and rates of weathering in cold and polar desert environments. In *Rates of Chemical Weathering of Rocks and Minerals* (ed. S. M. Colman and D. P. Dethier), pp. 193–235, Academic Press.

Viers J., Dupré B., Polvé M., Schott J., Dandurand J.-L., and Braun J.-J. (1997) Chemical weathering in the drainage basin of a tropical watershed (Nsimi-Zoetele site, Cameroon): comparison between organic-poor and organic-rich waters. *Chem. Geol.* **140,** 181–206.

Viers J., Dupré B., Braun J.-J., Deberdt S., Angeletti B., Ngoupayou J. D., and Michard A. (2000) Major and trace element abundances and strontium isotopes in the Nyong basin rivers (Cameroon): constraints on chemical weathering processes and elements transport mechanisms in humid tropical environments. *Chem. Geol.* **169,** 211–241.

Vogt K. A., Grier C. C., Meier C. E., and Edmonds R. L. (1982) Mycorrhizal role in net primary production and nutrient cycling in Abies amabilis ecosystems in westeren Washington. *Ecology* **63,** 370–380.

Vogt T. and Larqué P. (1998) Transformation and neoformations of clay in the cryogenic environment: examples from Transbaikalia (Siberia) and Patagonia (Argentina). *Eur. J. Soil Sci.* **49,** 367–376.

White A. F. and Blum A. E. (1995) Effects of climate on chemical weathering in watersheds. *Geochim. Cosmochim. Acta* **59,** 1729–1747.

White A. F., Bullen T. D., Davison V. V., Schulz M. S., and Clow D. W. (1999) The role of disseminated calcite in the chemical weathering of granitoid rocks. *Geochim. Cosmochim. Acta* **63,** 1939–1953.

White A. F., Schulz M. S., Lowenstern J. B., Vivit D. V., and Bullen T. D. (2005) The ubiquitous nature of accessory calcite in granitoid rocks: Implications for weathering, solute evolution and petrogenesis. *Geochim. Cosmochim. Acta* **69,** 1455–1471.

Zakharova E. A., Pokrovsky O. S., Dupré B., and Zaslavskaya M. B. (2005) Chemical weathering of silicate rocks in Aldan Shield and Baikal Uplift: insights from long-term seasonal measurements of solute fluxes in rivers. *Chem. Geol.* **214,** 223–248.

Zolotukhin V. V. and Al'Mukhamedov A. I. (1988) Traps of the Siberian Platform. In *Continental Flood Basalts* (ed. J. D. Macdougall), pp. 273–310, *Kluwer Academic Publishing*.

Zvereva T. S. and Ignatenko I. V. (1983) *Intra-Soil Weathering of Minerals in Tundra and Forest-Tundra.* Nauka Press (in Russian).

APPENDIX 1

Table A1. Parameters of Eqn. 1 and mean multiannual concentrations (C) for studied rivers. Uncertainty on average annual concentration is ±15–20%.

River, position on the map	Watershed, km^2	Runoff, mm/y	Element	k	n	r_{xy}	C, mg/L
N. Tunguska, Tura (A)	268,000	205 ± 15	Mg	82.6	−0.46	0.88	2.9
			Ca	800.5	−0.55	0.95	14.8
			Na + K	2949.0	−0.75	0.85	13.7
			HCO_3	551.4	−0.40	0.86	30.9
			SO_4	260.1	−0.49	0.71	4.9
			Cl	6341.9	−0.75	0.93	27.8
			Si	9.19	−0.082	0.31	4.0
N. Tunguska, Bolshoi Porog (D)	447,000	264 ± 2	Mg	68.4	−0.38	0.90	2.5
			Ca	1014.0	−0.51	0.95	12.1
			Na + K	3370.2	−0.67	0.90	9.6
			HCO_3	1486	−0.47	0.97	27.3
			SO_4	211.9	−0.36	0.77	4.9
			Cl	4617	−0.62	0.92	20.7
			Si	8.09	−0.094	0.21	4.6
Tembenchi (B, No 90)	18,900	434 ± 5	Mg	8.8	−0.33	0.82	1.4
			Ca	94.8	−0.45	0.88	7.8
			Na + K	73.1	−0.46	0.94	5.7
			HCO_3	50.9	−0.20	0.85	17.2
			SO_4	10.3	−0.16	0.29	4.9
			Cl	292.5	−0.61	0.95	10.1
			Si	6.11	−0.055	0.50	5.3
Eratchimo (E)	9,100	516 ± 5	Mg	42.7	−0.52	0.80	3.2
			Ca	153.9	−0.47	0.84	14.8
			Na + K	857.8	−0.74	0.92	21.0
			HCO_3	468.2	−0.49	0.88	41.1
			SO_4	90.2	−0.40	0.75	12.2
			Cl	1334.3	−0.74	0.91	33.0
			Si	8.31	−0.096	0.44	3.1
Taimura (C, No 5)	15,600	205 ± 15	Mg	8.3	−0.21	0.91	3.2
			Ca	69.4	−0.34	0.86	15.2
			Na + K	86.1	−0.44	0.88	12.0
			HCO_3	157.5	−0.28	0.79	45.7
			SO_4	37.5	−0.24	0.64	12.7
			Cl	137.8	−0.44	0.91	19.5
			Si	8.31	−0.096	0.44	5.8

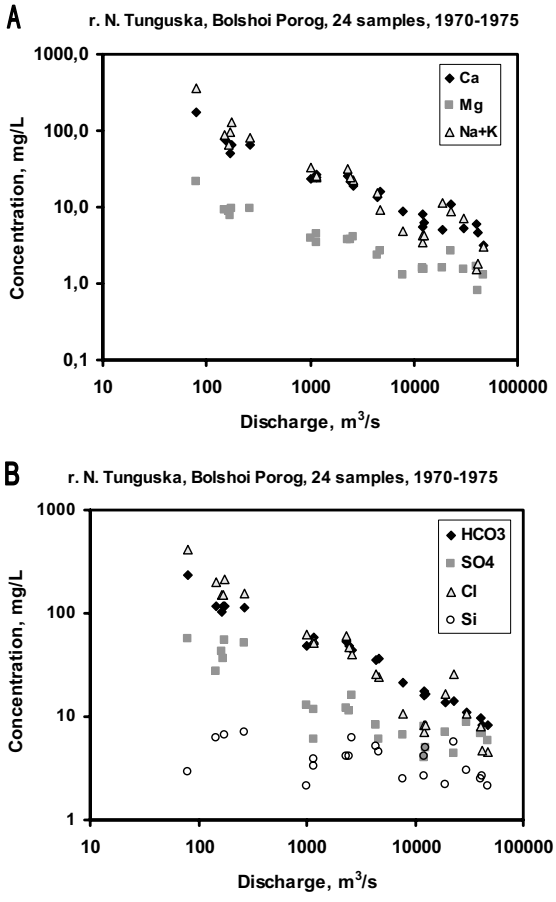

Fig. A1-1. Concentrations of Ca, Mg, Na + K (A) and HCO_3, Cl, SO_4, Si (B) as a function of discharge for N. Tunguska River at Bolshoi Porog (sample D on the map of Fig. 1).

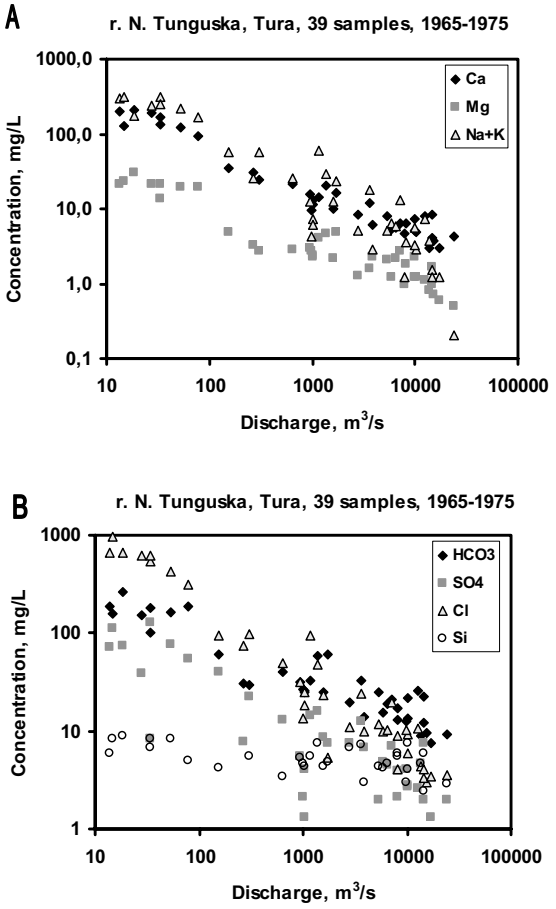

Fig. A1-2. Concentrations of Ca, Mg, Na + K (A) and HCO_3, Cl, SO_4, Si (B) as a function of discharge for N. Tunguska River at Tura town (sample A on the map of Fig. 1).

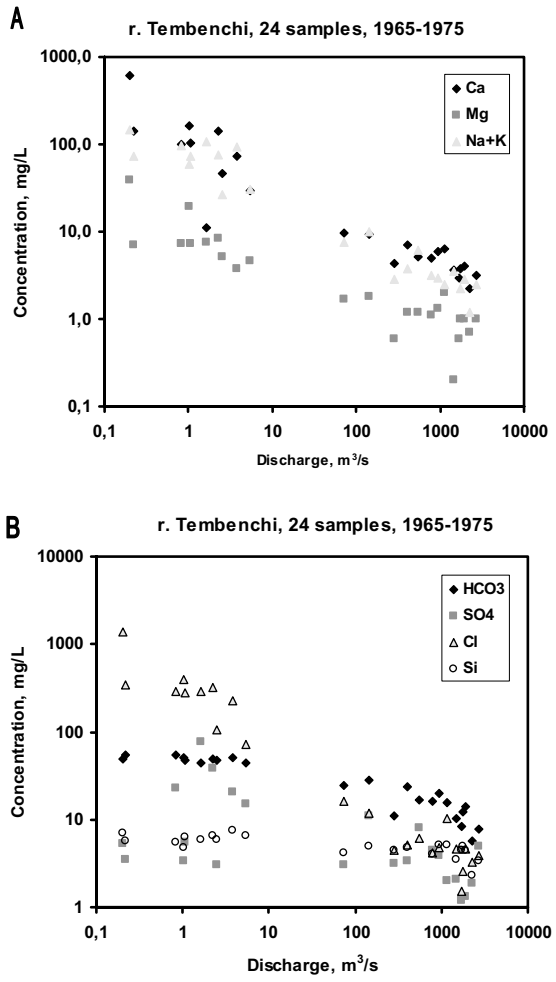

Fig. A1-3. Concentrations of Ca, Mg, Na + K (A) and HCO_3, Cl, SO_4, Si (B) as a function of discharge for Tembenchi River (sample B, No 90 on the map of Fig. 1).

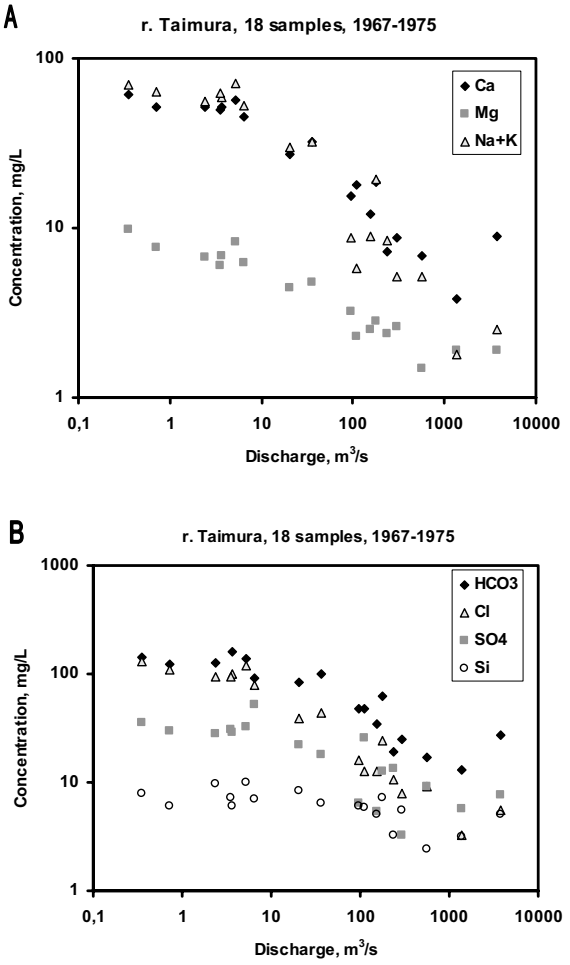

Fig. A1-4. Concentrations of Ca, Mg, Na + K (A) and HCO_3, Cl, SO_4, Si (B) as a function of discharge for Teimura River (sample C, No 5 on the map of Fig. 1).

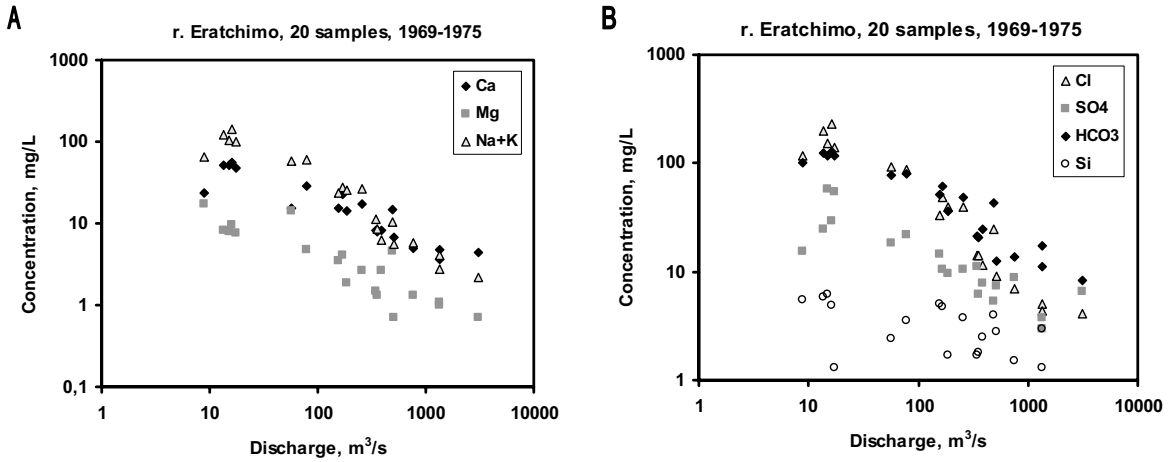

Fig. A1-5. Concentrations of Ca, Mg, Na + K (A) and HCO_3, Cl, SO_4, Si (B) as a function of discharge for Eratchimo River (sample E, on the map of Fig. 1).

APPENDIX 2

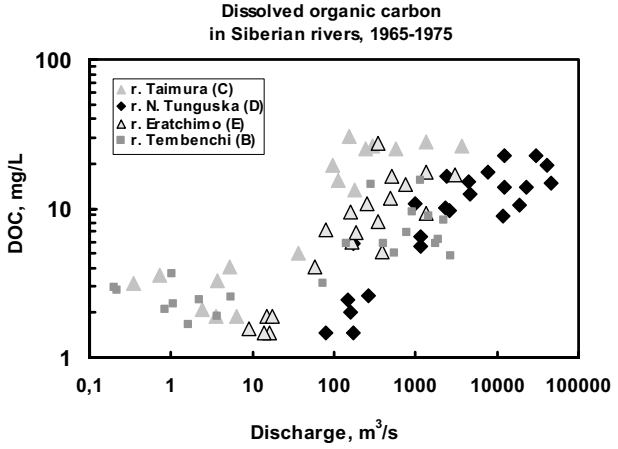

Fig. A2. Dissolved organic carbon concentration for four rivers of the Hydrological Survey database as a function of discharge over the year.